# Probing the Variation of the Intervalley Tunnel Coupling in a Silicon Triple Quantum Dot

F. Borjans, X. Zhang, X. Mi, G. Cheng, N. Yao, C.A.C. Jackson, L.F. Edge and J.R. Petta (PRX Quantum 2, 2021)

**Journal Club of the NCCR spin on May 16 2022**

**JH Ungerer**

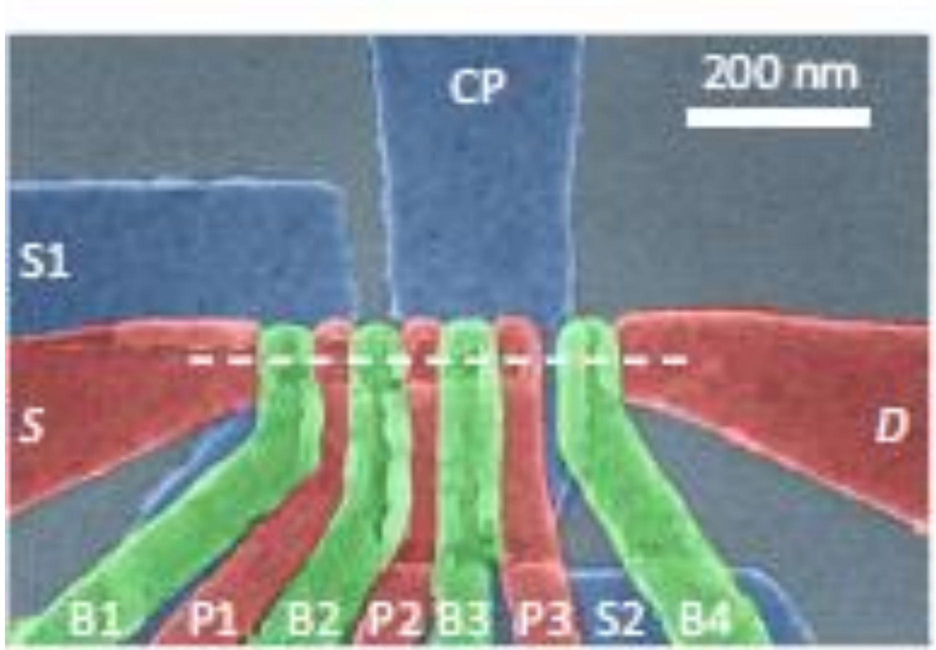


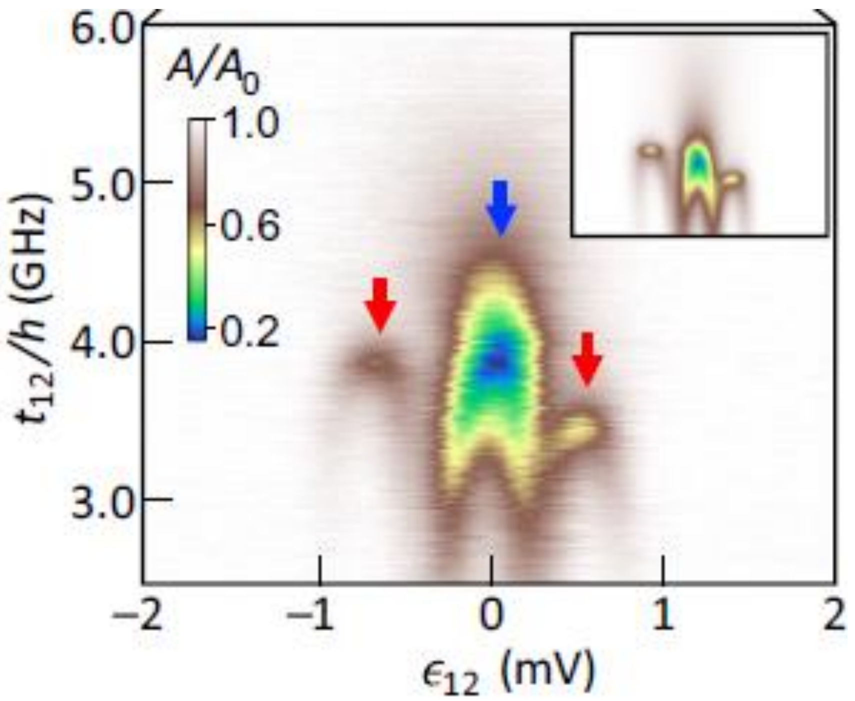

# Motivation

- **Valley degree of freedom of electrons in Silicon**
  - Valley-orbit coupling can limit spin lifetime and inhibit coherent electron shuffeling

# Motivation

- **Valley degree of freedom of electrons in Silicon**
    - Valley-orbit coupling can limit spin lifetime and inhibit coherent electron shuffeling
    - Measuring the valley splitting gives insights into the quality of the crystal growth

# Motivation

- **Valley degree of freedom of electrons in Silicon**
  - Valley-orbit coupling can limit spin lifetime and inhibit coherent electron shuffeling
  - Measuring the valley splitting gives insights into the quality of the crystal growth
- **Circuit QED for determining valley splitting**
  - Resonator sensitive to avoided crossings due to intra- and inter valley tunneling

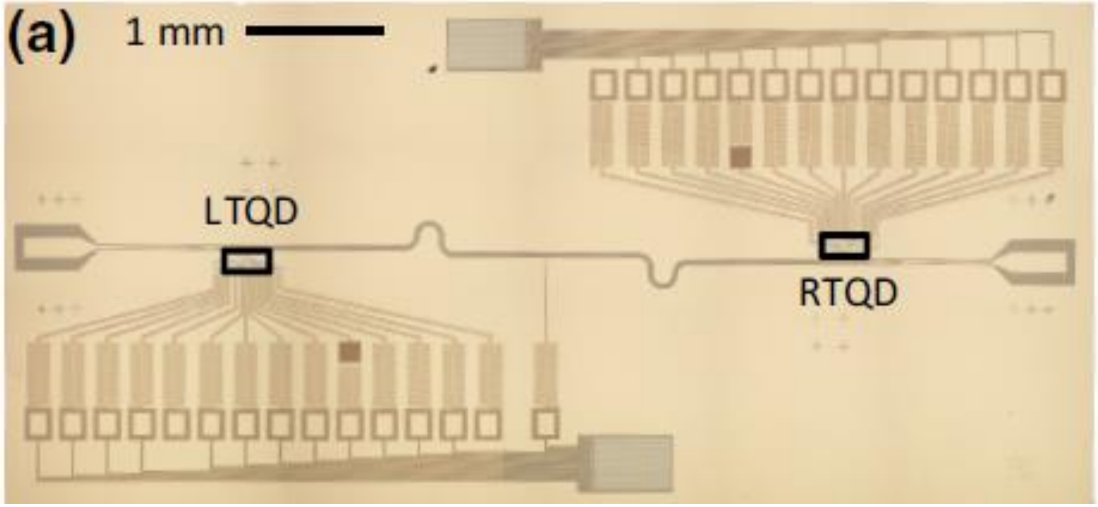

# Valley degree of freedom in silicon quantum dots

- Diamond cubic crystal structure
- Six degenerate CB minima (valleys)

First Brillouin zone

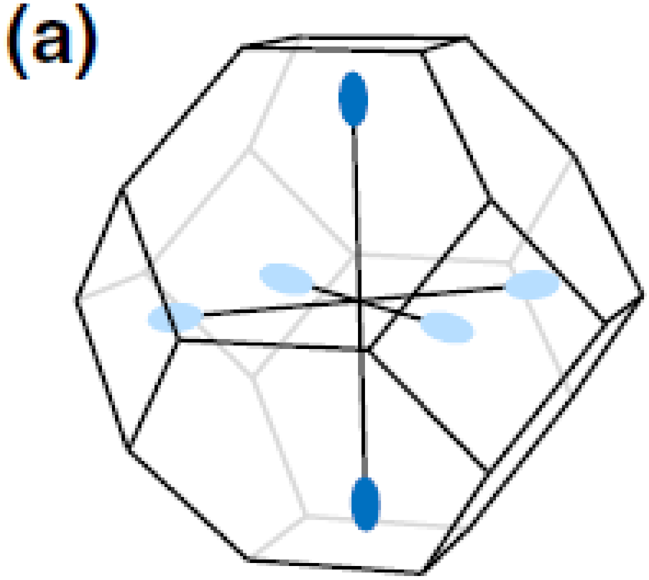


Band structure of silicon

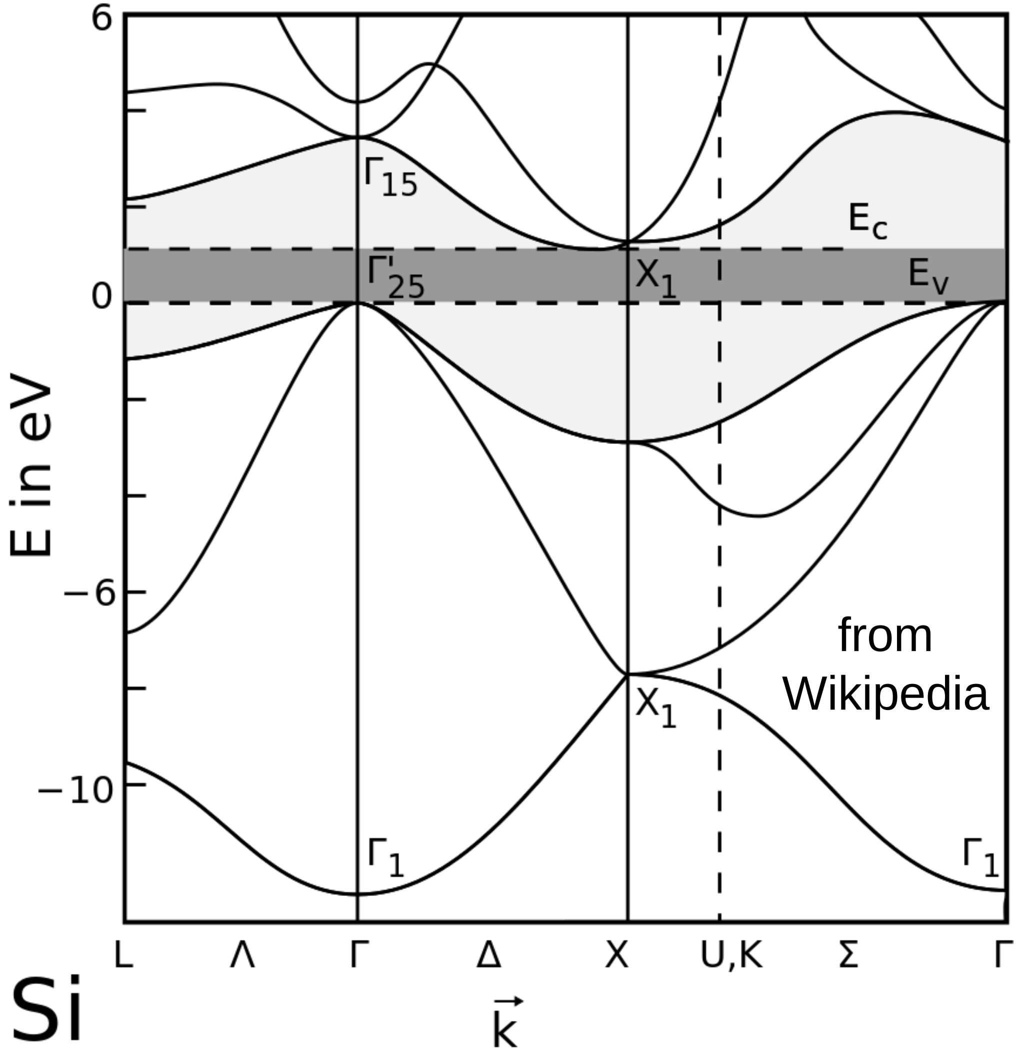


from Wikipedia

# Valley degree of freedom in silicon quantum dots

- **Tensile strain of quantum well**
  - Increased energy of $\pm X, \pm Y$ valleys

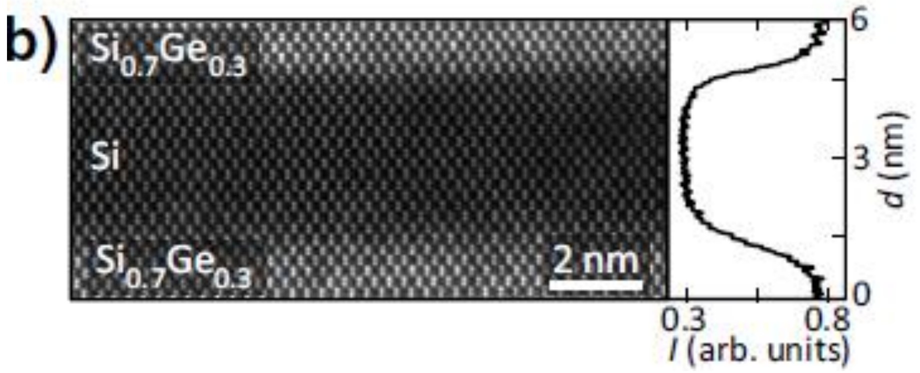


First Brillouin zone

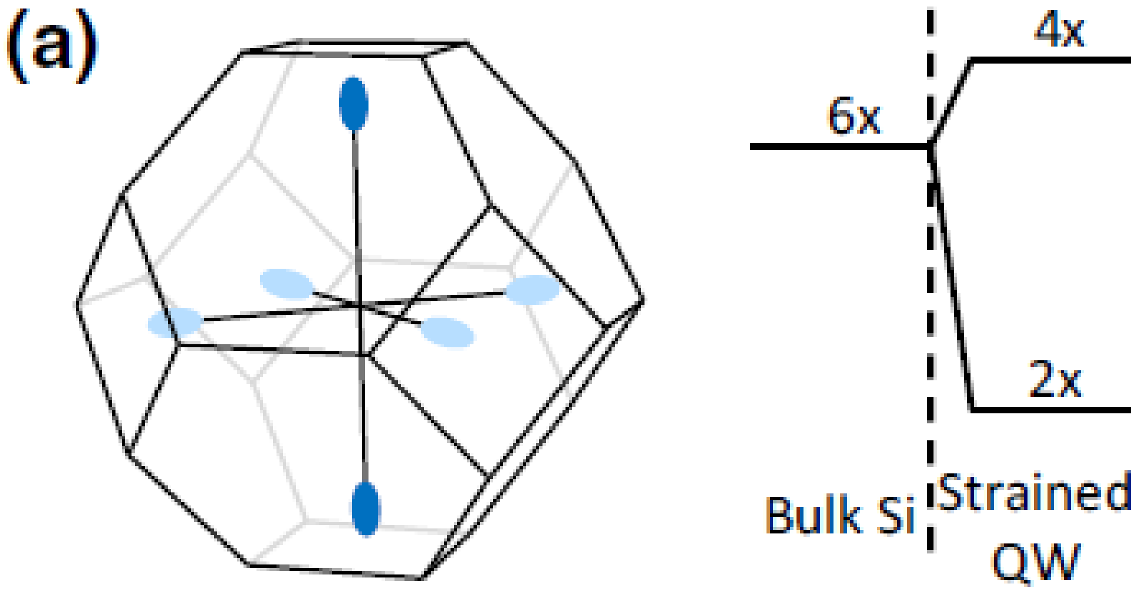

# Valley degree of freedom in silicon quantum dots

- **Tensile strain of quantum well**
  - Increased energy of $\pm X, \pm Y$ valleys
- **Break of inversion symmetry (confinment)**
  - Lifted degeneracy of $\pm Z$

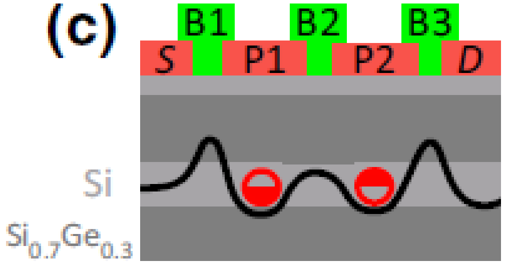


First Brillouin zone

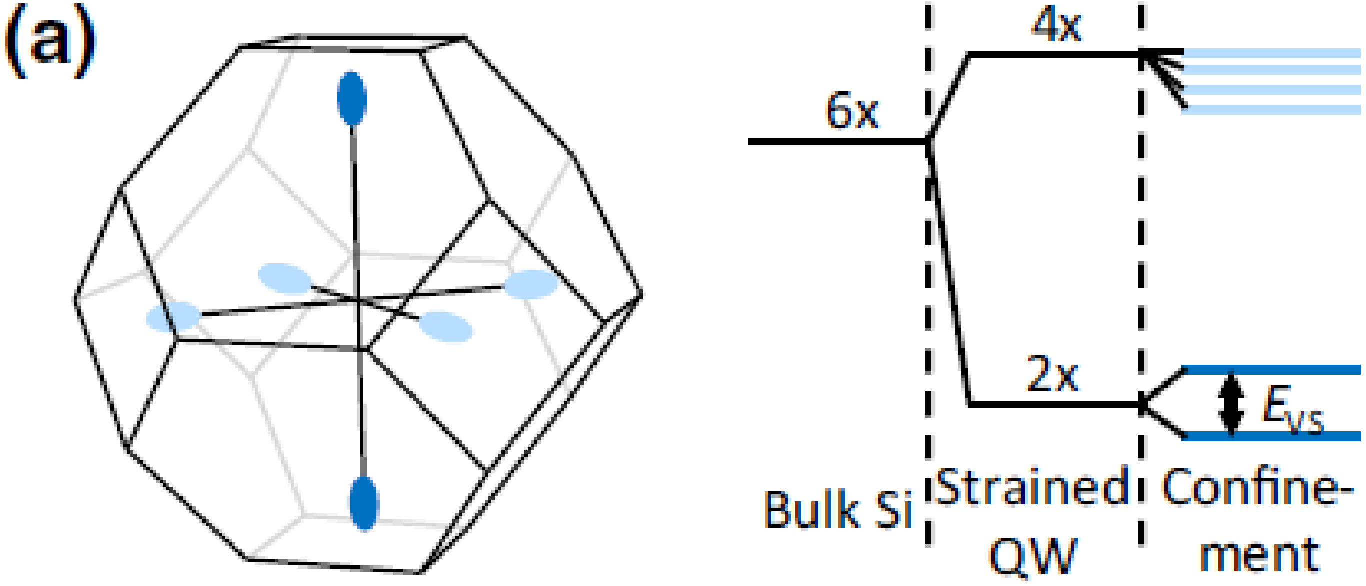

# Valley degree of freedom in silicon quantum dots

- **Tensile strain of quantum well**
  - Increased energy of $\pm X, \pm Y$ valleys
- **Break of inversion symmetry (confinement)**
  - Lifted degeneracy of $\pm Z$
- **Imperfect, soft interfaces and step edges**
  - Inter-valley tunneling

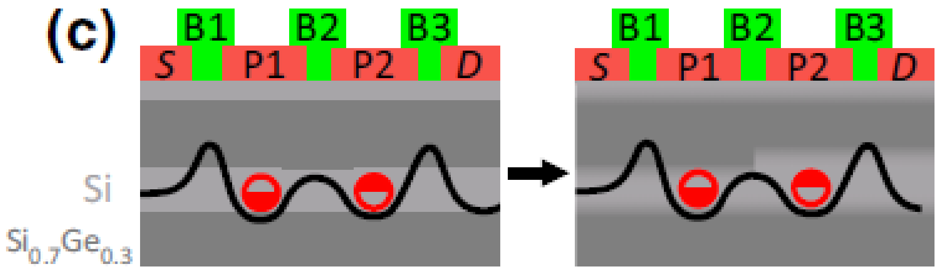


First Brillouin zone

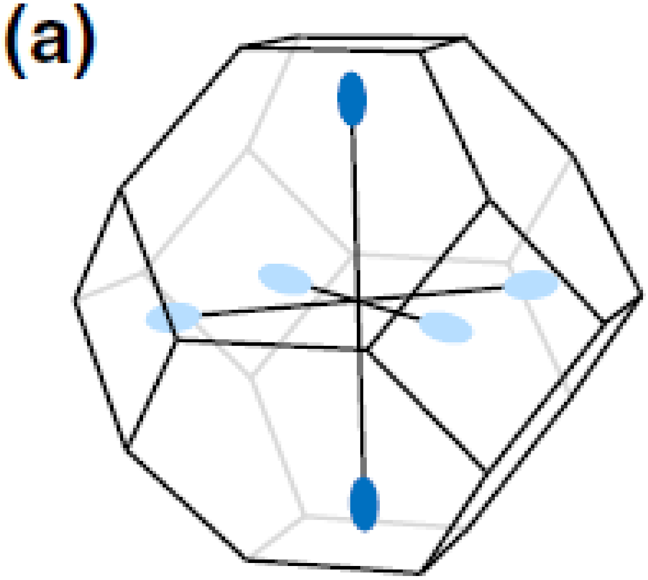


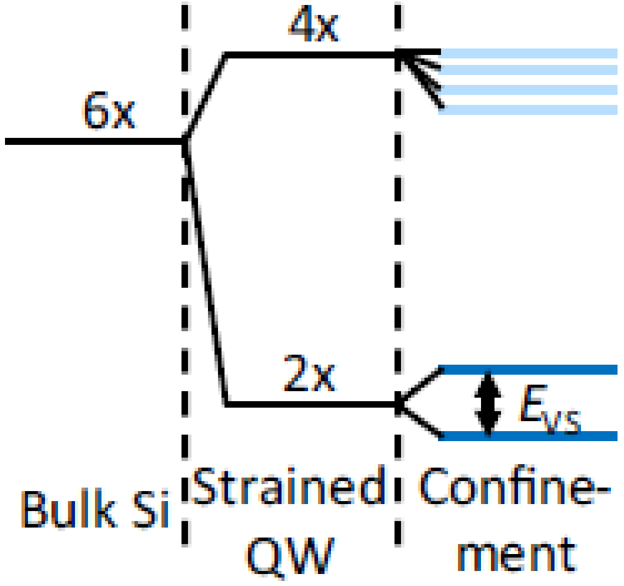

# Valley degree of freedom in silicon quantum dots

- **Hamiltonian of 1-dot subsystem**

$$H_{V,i} = \begin{pmatrix} 0 & \Delta_i \\ \Delta_i^* & 0 \end{pmatrix}$$

Basis:

$\{|i, +z\rangle, |i, -z\rangle\}$

$\Delta = |\Delta| e^{i\Phi}$ valley coupling

# Valley degree of freedom in silicon quantum dots

- **Hamiltonian of 1-dot subsystem**

$$H_{V,i} = \begin{pmatrix} 0 & \Delta_i \\ \Delta_i^* & 0 \end{pmatrix}$$

Basis:
$\{|i,+z\rangle, |i,-z\rangle\}$
$\Delta = |\Delta| e^{i\Phi}$ valley coupling

- **Hamiltonian of DOD**

$$H_{ij}(\epsilon_{ij}) = \begin{pmatrix} \frac{\epsilon_{ij}}{2} & \Delta_i & t_c & 0 \\ \Delta_i^* & \frac{\epsilon_{ij}}{2} & 0 & t_c \\ t_c & 0 & -\frac{\epsilon_{ij}}{2} & \Delta_j \\ 0 & t_c & \Delta_j^* & -\frac{\epsilon_{ij}}{2} \end{pmatrix}$$

Basis:
$\{|i,+z\rangle, |i,-z\rangle, |j,+z\rangle, |j,-z\rangle\}$

$t_c$ = dot-dot tunneling
$\epsilon$ = dot-dot detuning

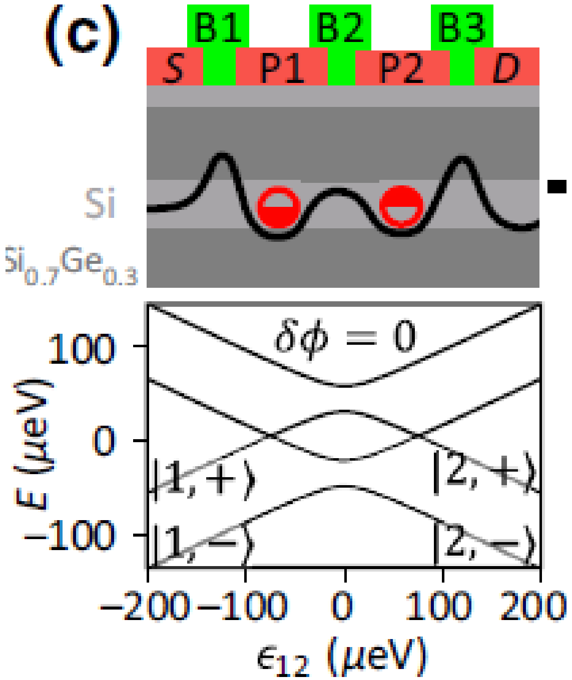

# Valley degree of freedom in silicon quantum dots

- **Hamiltonian of 1-dot subsystem**

$$H_{V,i} = \begin{pmatrix} 0 & \Delta_i \\ \Delta_i^* & 0 \end{pmatrix}$$

Basis:
$\{|i,+z\rangle, |i,-z\rangle\}$
$\Delta = |\Delta| e^{i\Phi}$ valley coupling

- **Hamiltonian of DOD**

$$H_{ij}(\epsilon_{ij}) = \begin{pmatrix} \frac{\epsilon_{ij}}{2} & \Delta_i & t_c & 0 \\ \Delta_i^* & \frac{\epsilon_{ij}}{2} & 0 & t_c \\ t_c & 0 & -\frac{\epsilon_{ij}}{2} & \Delta_j \\ 0 & t_c & \Delta_j^* & -\frac{\epsilon_{ij}}{2} \end{pmatrix}$$

Basis:
$\{|i,+z\rangle, |i,-z\rangle, |j,+z\rangle, |j,-z\rangle\}$

$t_c$ = dot-dot tunneling
$\epsilon$ = dot-dot detuning

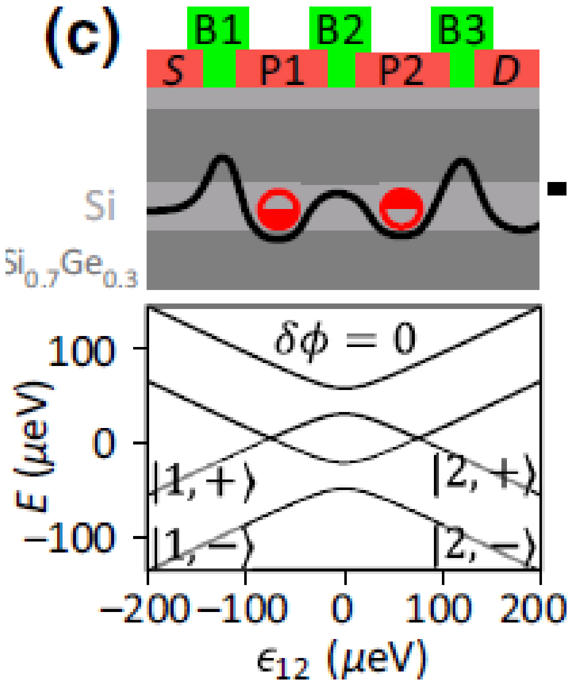


- **After diagonalizing the single-dot part**

$$H'_{ij}(\epsilon_{ij}) = \begin{pmatrix} \frac{\epsilon_{ij}}{2} + E_{\mathrm{VS},i} & 0 & t_{ij} & t'_{ij} \\ 0 & \frac{\epsilon_{ij}}{2} & t'_{ij} & t_{ij} \\ t^*_{ij} & t'^*_{ij} & -\frac{\epsilon_{ij}}{2} + E_{\mathrm{VS},j} & 0 \\ t'^*_{ij} & t^*_{ij} & 0 & -\frac{\epsilon_{ij}}{2} \end{pmatrix}$$

Basis:
$\{|i,+\rangle, |i,-\rangle, |j,+\rangle, |j,-\rangle\}$

Intra-valley tunneling
$$t_{ij} = (1/2)t_c(1 + e^{-i\delta\phi_{ij}})$$
Inter-valley tunneling
$$t'_{ij} = (1/2)t_c(1 - e^{-i\delta\phi_{ij}})$$

# Valley degree of freedom in silicon quantum dots

- **Hamiltonian of 1-dot subsystem**

$$H_{V,i} = \begin{pmatrix} 0 & \Delta_i \\ \Delta_i^* & 0 \end{pmatrix}$$

Basis:
$\{|i,+z\rangle, |i,-z\rangle\}$
$\Delta = |\Delta| e^{i\Phi}$ valley coupling

- **Hamiltonian of DOD**

$$H_{ij}(\epsilon_{ij}) = \begin{pmatrix} \frac{\epsilon_{ij}}{2} & \Delta_i & t_c & 0 \\ \Delta_i^* & \frac{\epsilon_{ij}}{2} & 0 & t_c \\ t_c & 0 & -\frac{\epsilon_{ij}}{2} & \Delta_j \\ 0 & t_c & \Delta_j^* & -\frac{\epsilon_{ij}}{2} \end{pmatrix}$$

Basis:
$\{|i,+z\rangle, |i,-z\rangle, |j,+z\rangle, |j,-z\rangle\}$

$t_c$ = dot-dot tunneling
$\epsilon$ = dot-dot detuning

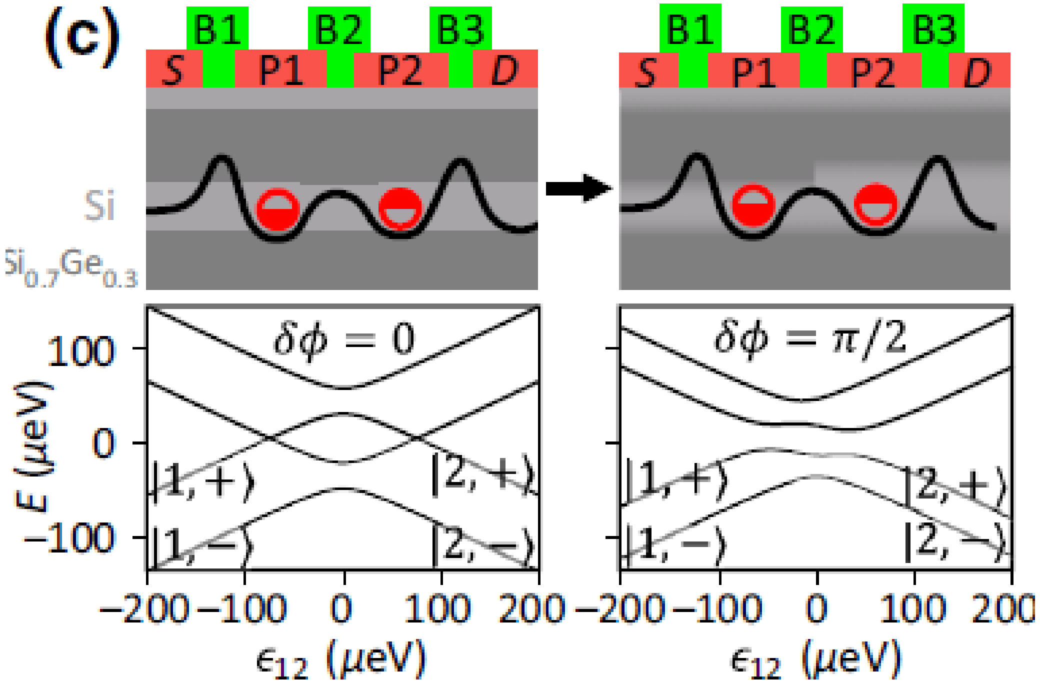


- **After diagonalizing the single-dot part**

$$H'_{ij}(\epsilon_{ij}) = \begin{pmatrix} \frac{\epsilon_{ij}}{2} + E_{\mathrm{VS},i} & 0 & t_{ij} & t'_{ij} \\ 0 & \frac{\epsilon_{ij}}{2} & t'_{ij} & t_{ij} \\ t^*_{ij} & t'^*_{ij} & -\frac{\epsilon_{ij}}{2} + E_{\mathrm{VS},j} & 0 \\ t'^*_{ij} & t^*_{ij} & 0 & -\frac{\epsilon_{ij}}{2} \end{pmatrix}$$

Basis:
$\{|i,+\rangle, |i,-\rangle, |j,+\rangle, |j,-\rangle\}$

Intra-valley tunneling
$$t_{ij} = (1/2)t_c(1 + \boxed{e^{-i\delta\phi_{ij}}})$$
Inter-valley tunneling
$$t'_{ij} = (1/2)t_c(1 - \boxed{e^{-i\delta\phi_{ij}}})$$

Valley phase difference, because of valley orbit coupling
$\Delta = \Delta(x);\ \Delta_i \neq \Delta j$

# Experimental Setup

- Half wave CPW resonator coupled to TQD, $f_r = 6.76$ GHz $\kappa/2\pi = 1.5$ MHz

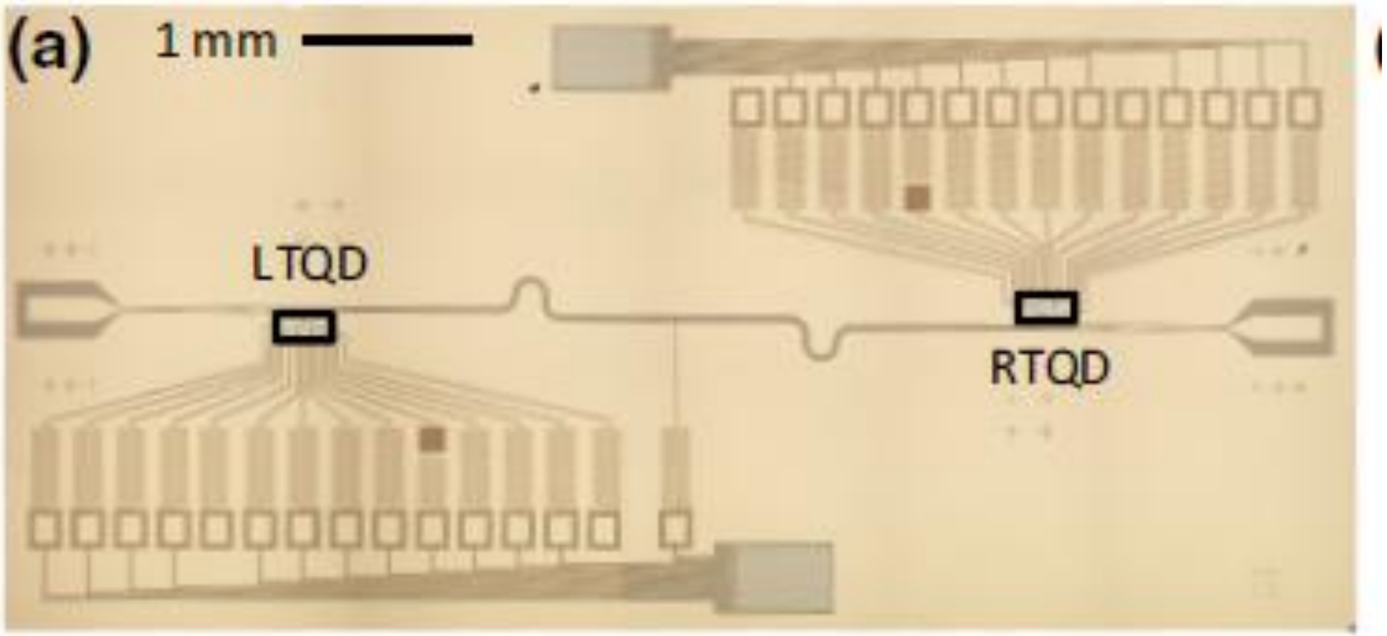

# Experimental Setup

- Half wave CPW resonator coupled to TQD, $f_r = 6.76$ GHz $\kappa/2\pi = 1.5$ MHz
- 3 overlapping Al gate layers separated by native $Al_2O_3$

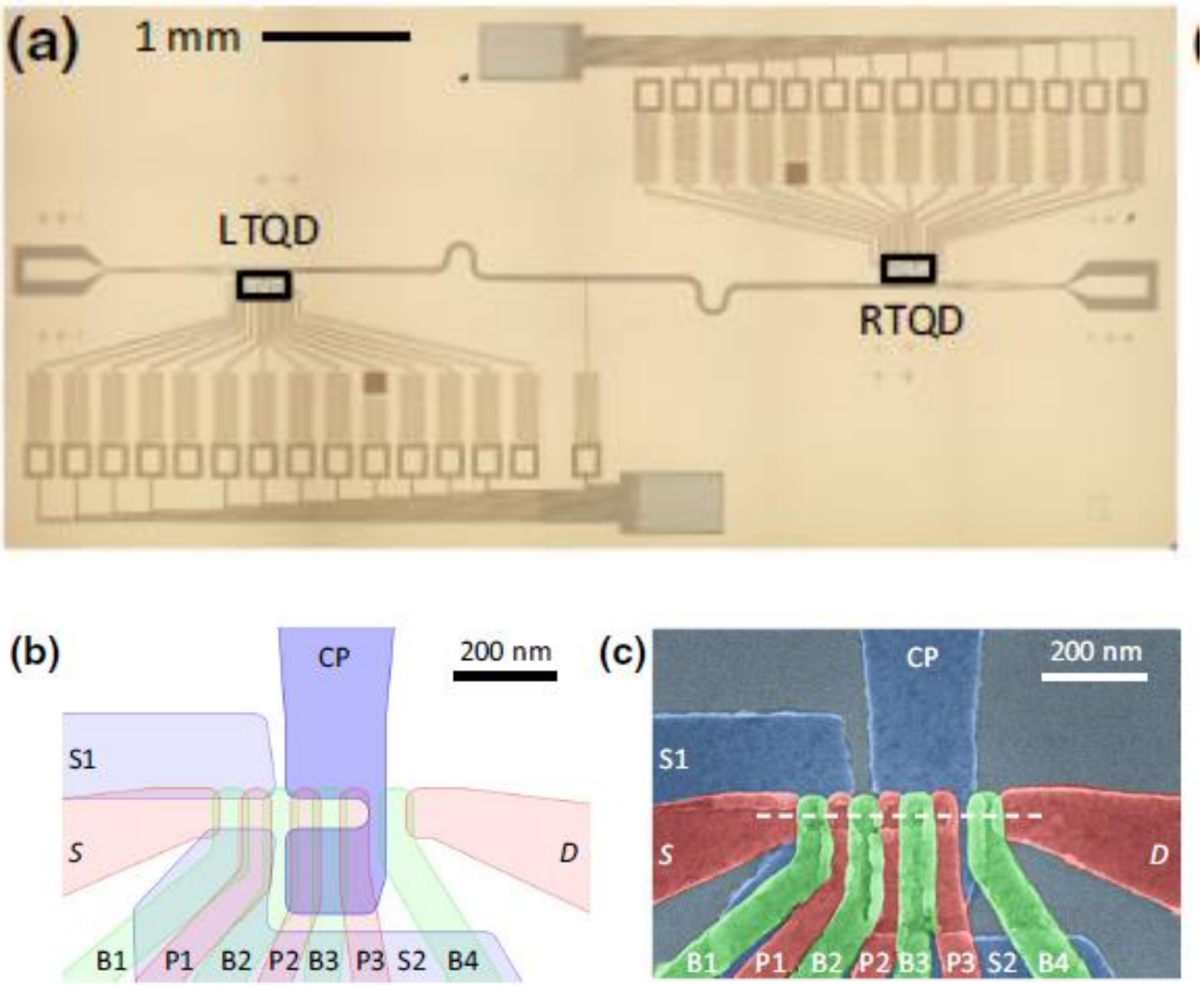

# Experimental Setup

- Half wave CPW resonator coupled to TQD, $f_r = 6.76$ GHz $\kappa/2\pi = 1.5$ MHz
- 3 overlapping Al gate layers separated by native $Al_2O_3$
- CP gate wraps around dot 3 to enhance dot-resonator coupling

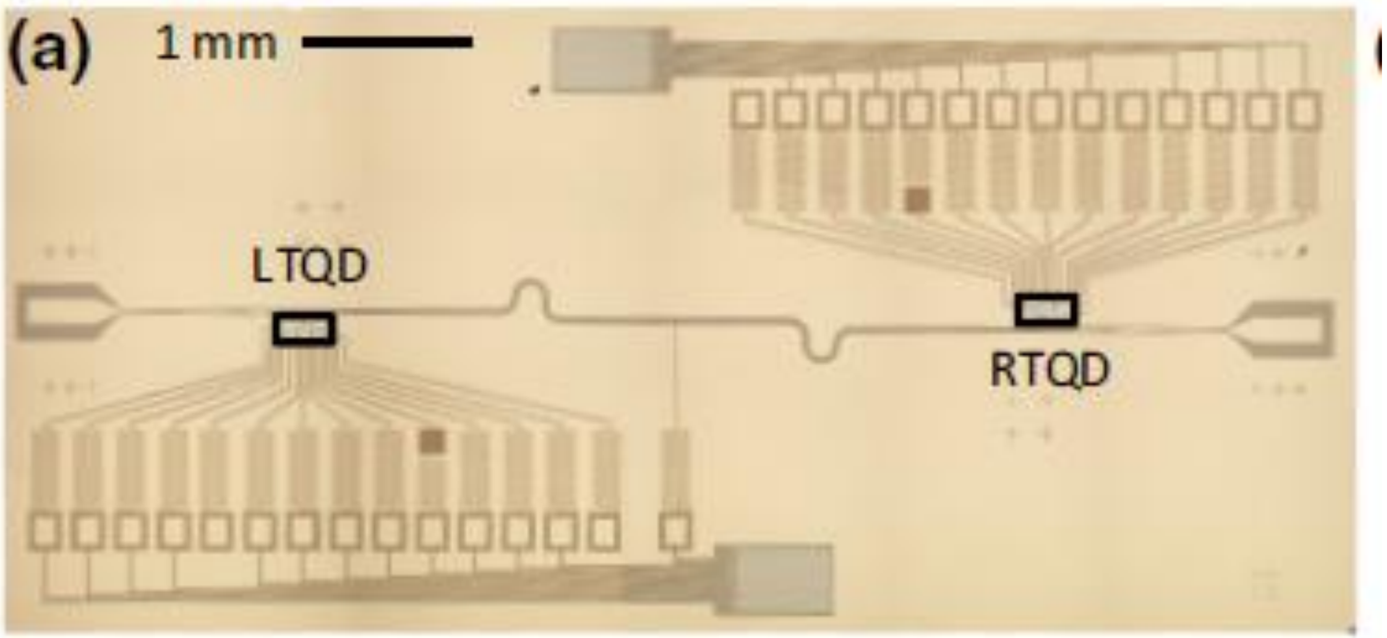


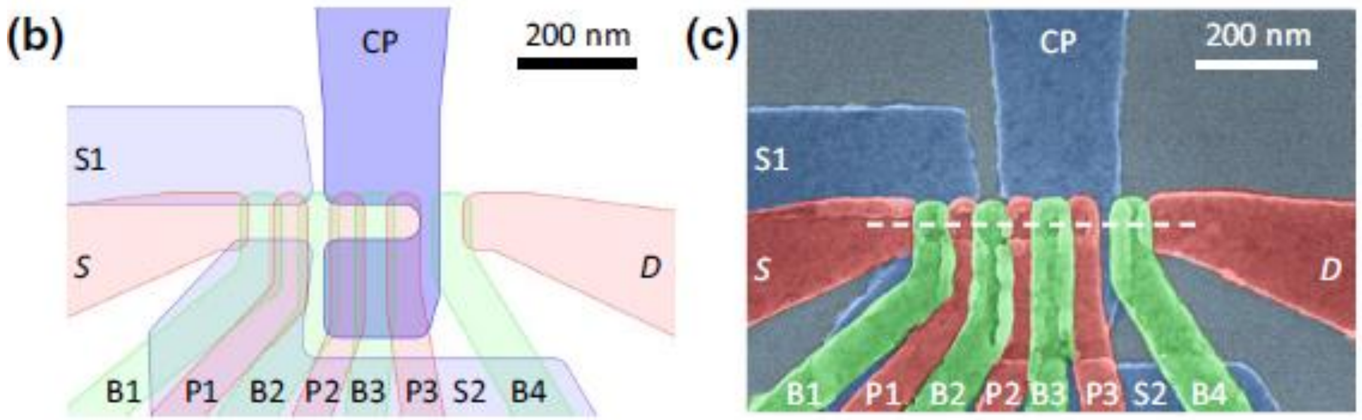

# Tuning towards last electron in TQD

- Read-out of resonator that is sensitive to charge transitions

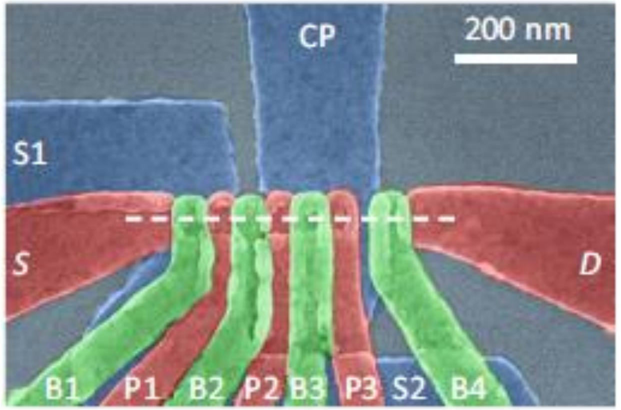


Dot 3 empty

Dot 1 filled to extend lead

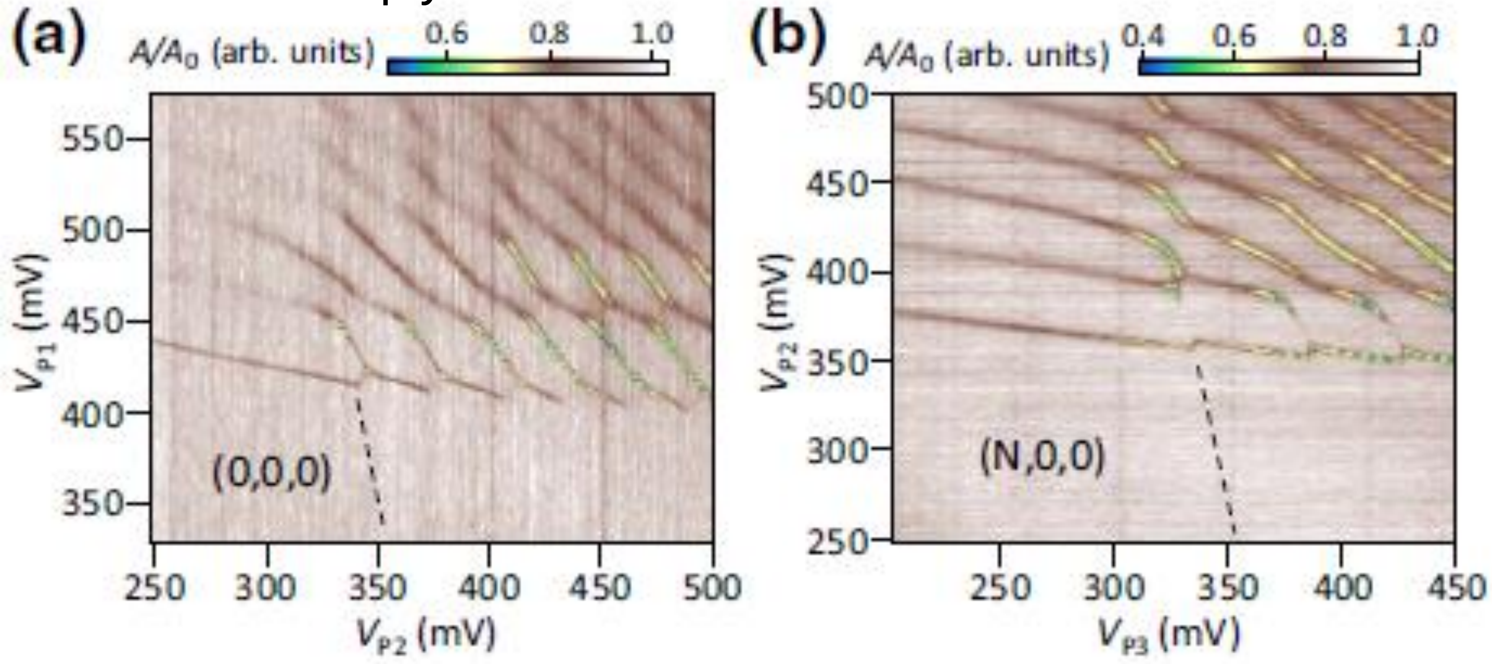

# Tuning towards last electron in TQD

- Read-out of resonator that is sensitive to charge transitions

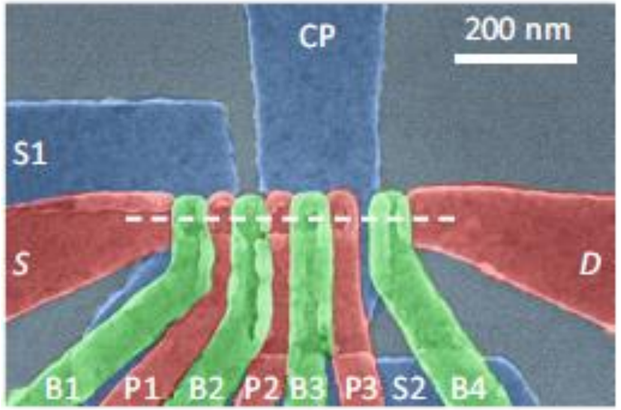


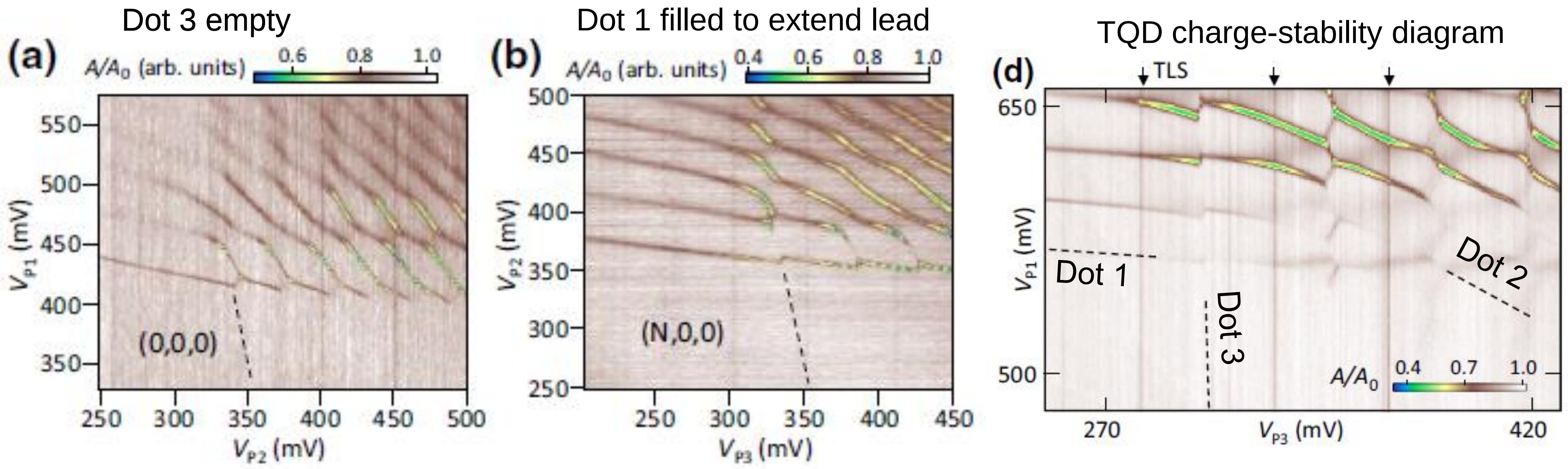

# Operation at last electron in the TQD

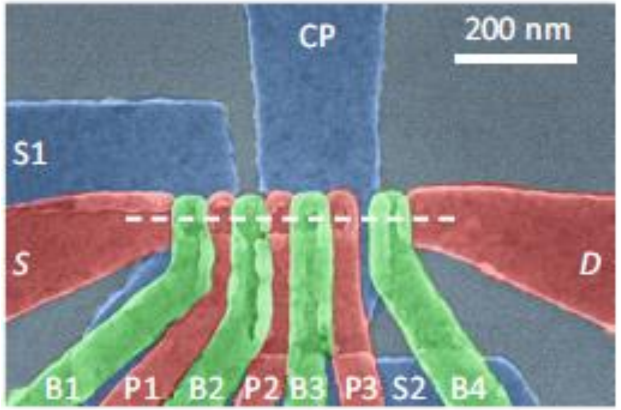


Operation point in transformed gate axes

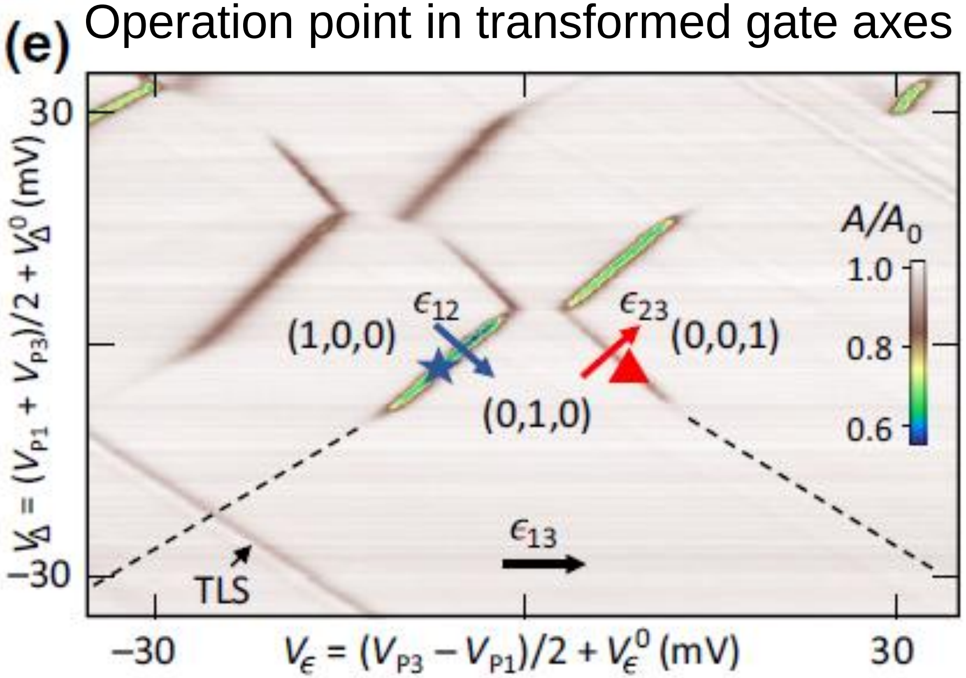


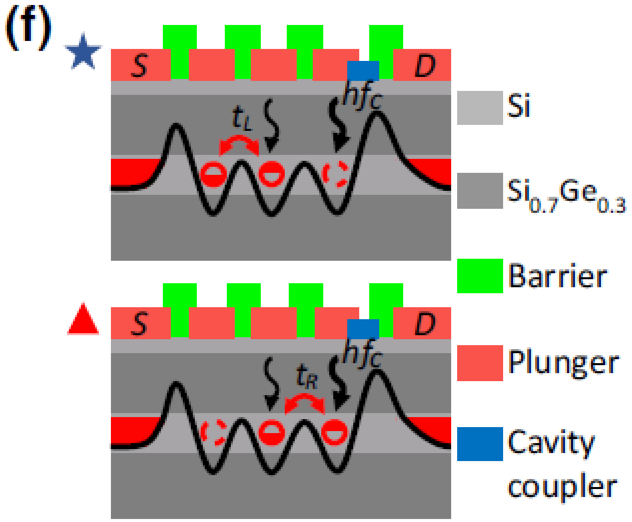

# Spectroscopic measurement of the valley states

- Sweep barrier versus detuning

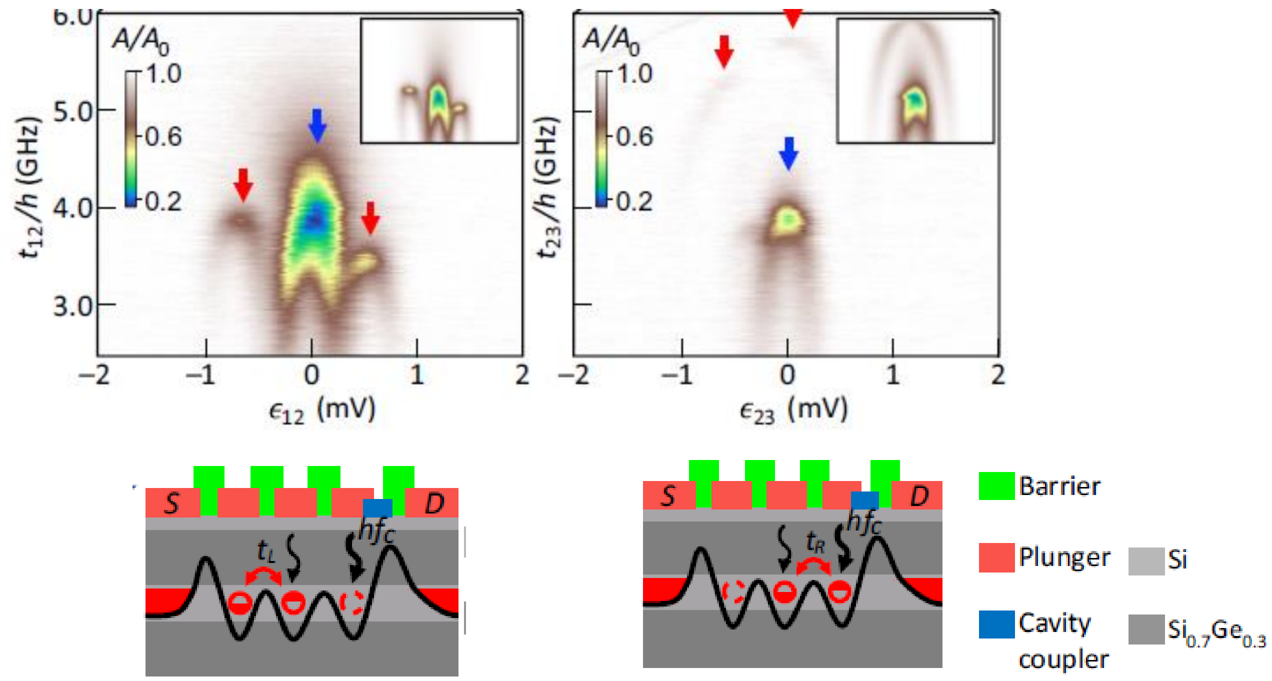

# Spectroscopic measurement of the valley states

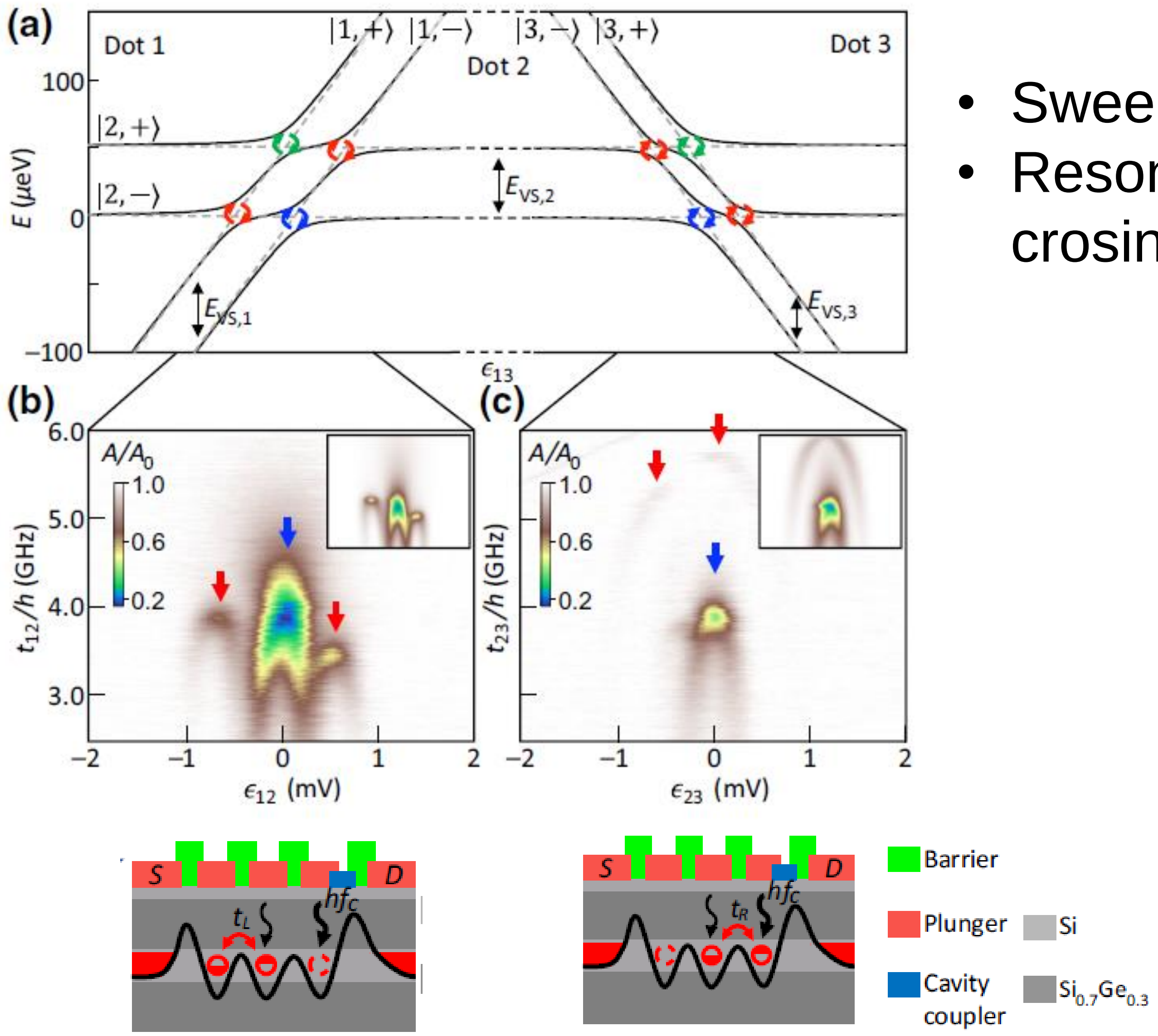


- Sweep barrier versus detuning
- Resonator sensitive to curvature at avoided crosings

# Spectroscopic measurement of the valley states

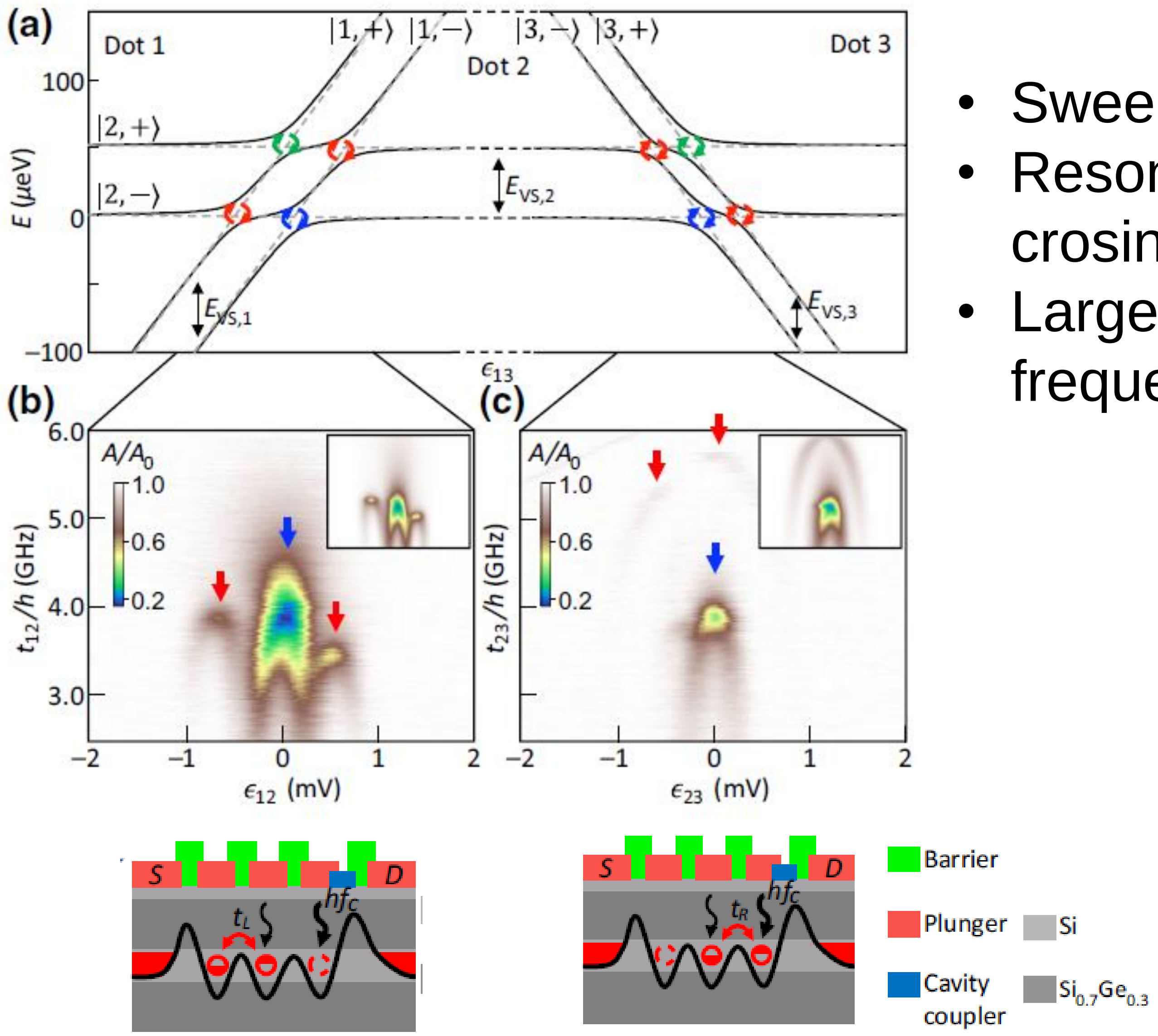


- Sweep barrier versus detuning
- Resonator sensitive to curvature at avoided crosings
- Largest resonator response when transition frequencies are close to resonator frequency

# Spectroscopic measurement of the valley states

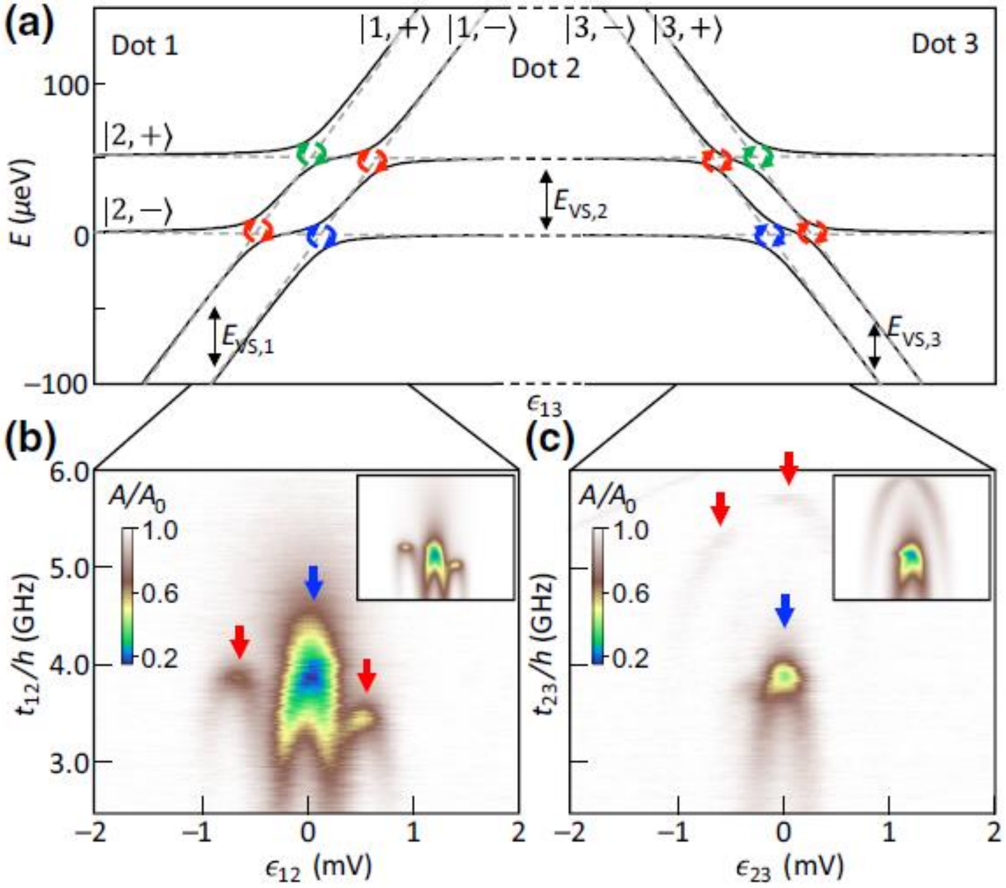


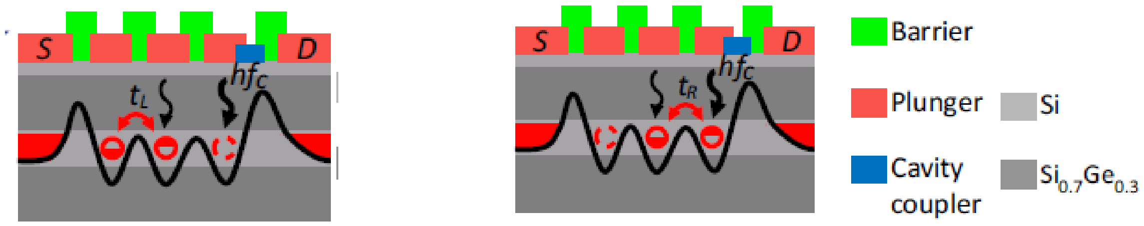


- Sweep barrier versus detuning
- Resonator sensitive to curvature at avoided crosings
- Largest resonator response when transition frequencies are close to resonator frequency
- Operation temperature $T_e = 350$ mK enables sensing of higher lying transitions

# Spectroscopic measurement of the valley states

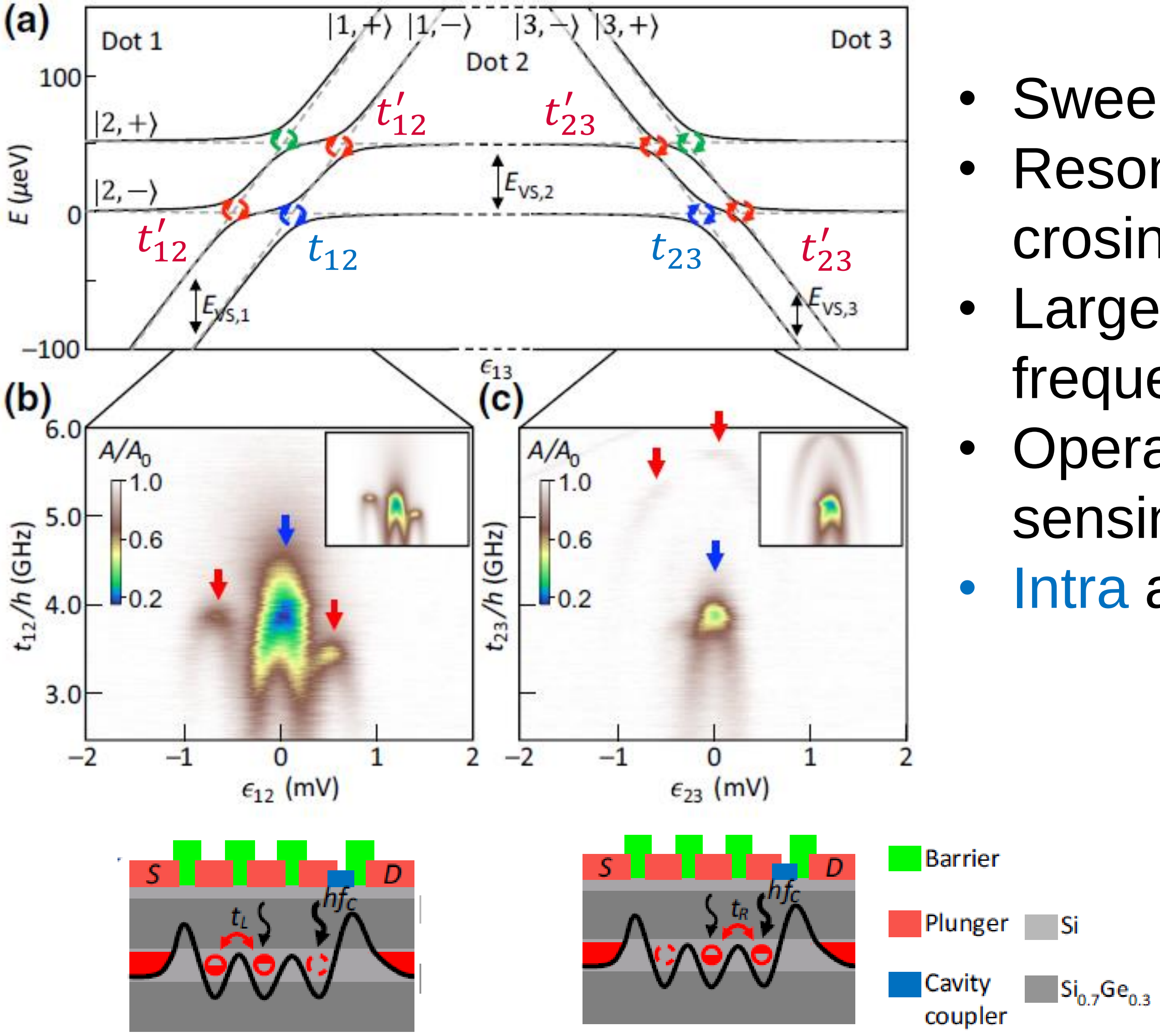


- Sweep barrier versus detuning
- Resonator sensitive to curvature at avoided crossings
- Largest resonator response when transition frequencies are close to resonator frequency
- Operation temperature $T_e = 350$ mK enables sensing of higher lying transitions
- Intra and inter-valley crossings are detected

# Spectroscopic measurement of the valley states

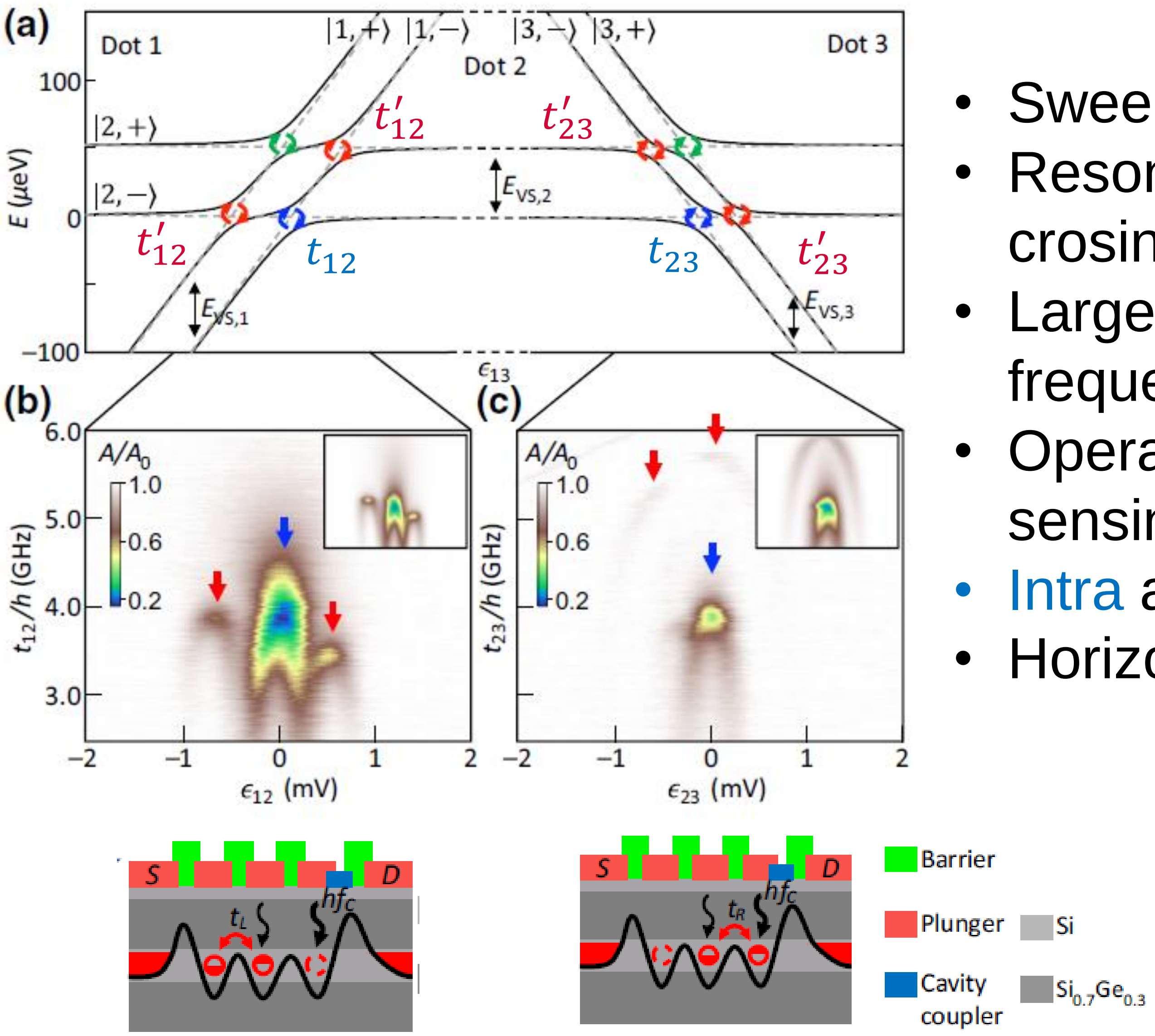


- Sweep barrier versus detuning
- Resonator sensitive to curvature at avoided crosings
- Largest resonator response when transition frequencies are close to resonator frequency
- Operation temperature $T_e = 350$ mK enables sensing of higher lying transitions
- Intra and inter-valley crossings are detected
- Horizontal positioning of archs due to $E_{V,i}$

# Spectroscopic measurement of the valley states

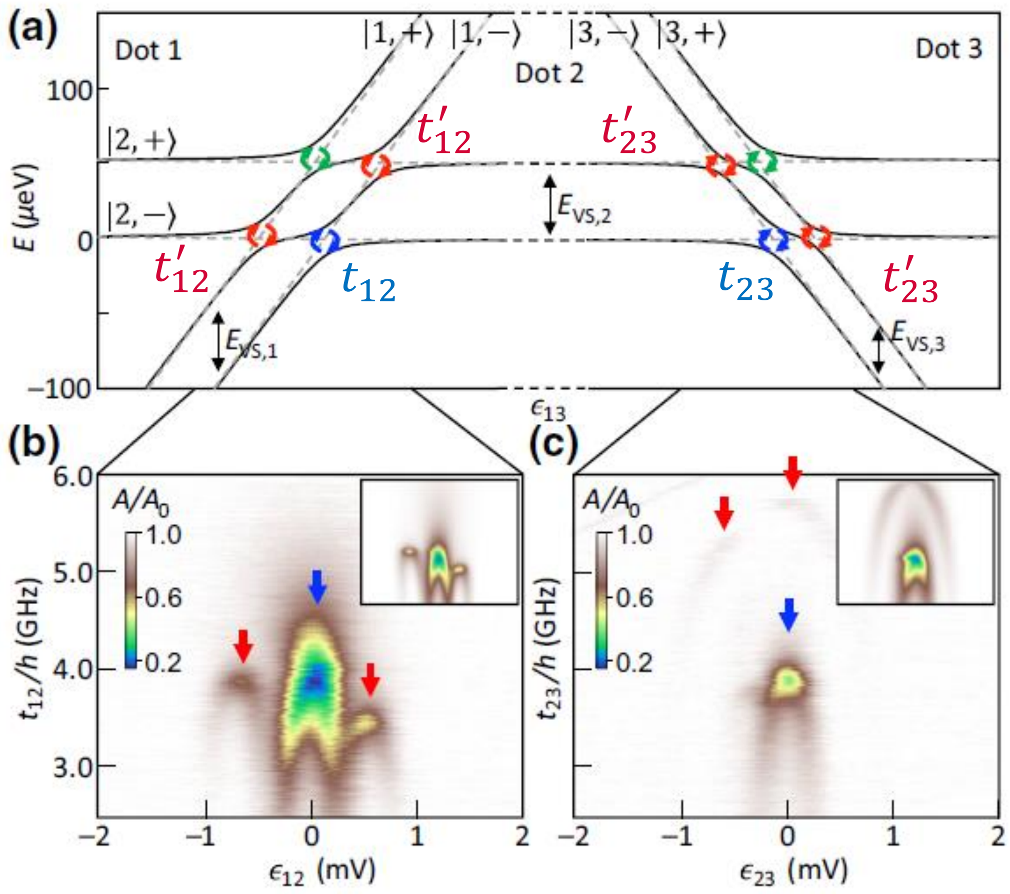


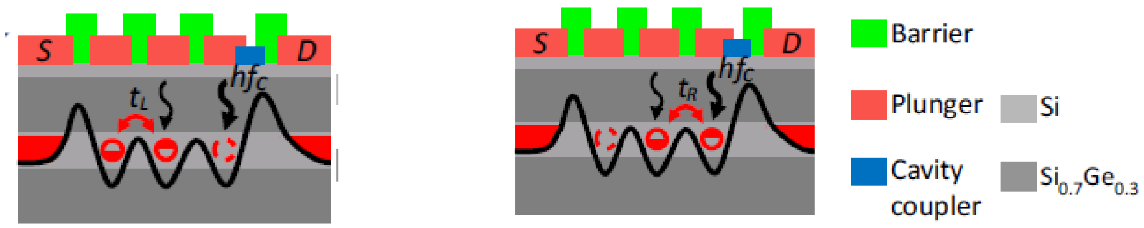


- Sweep barrier versus detuning
- Resonator sensitive to curvature at avoided crosings
- Largest resonator response when transition frequencies are close to resonator frequency
- Operation temperature $T_e = 350$ mK enables sensing of higher lying transitions
- Intra and inter-valley crossings are detected
- Horizontal positioning of archs due to $E_{V,i}$
- Vertical spacing of archs sugests $t'_{ij} = t'_{ij}(\epsilon)$

# Quantitative data analysis

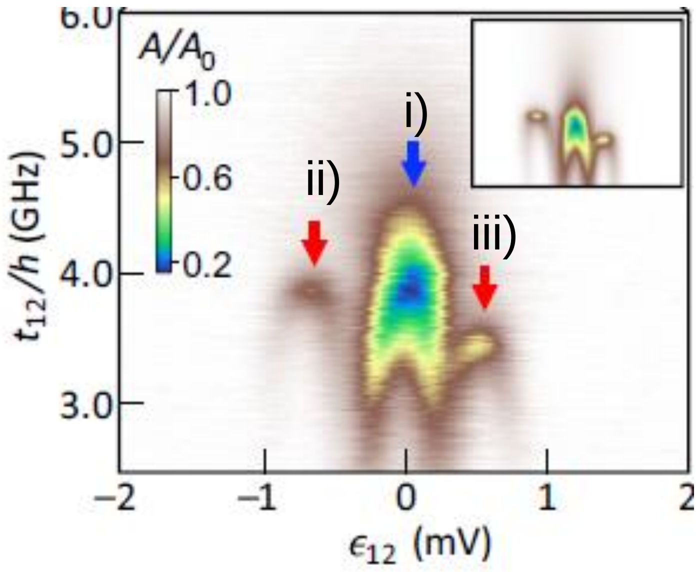


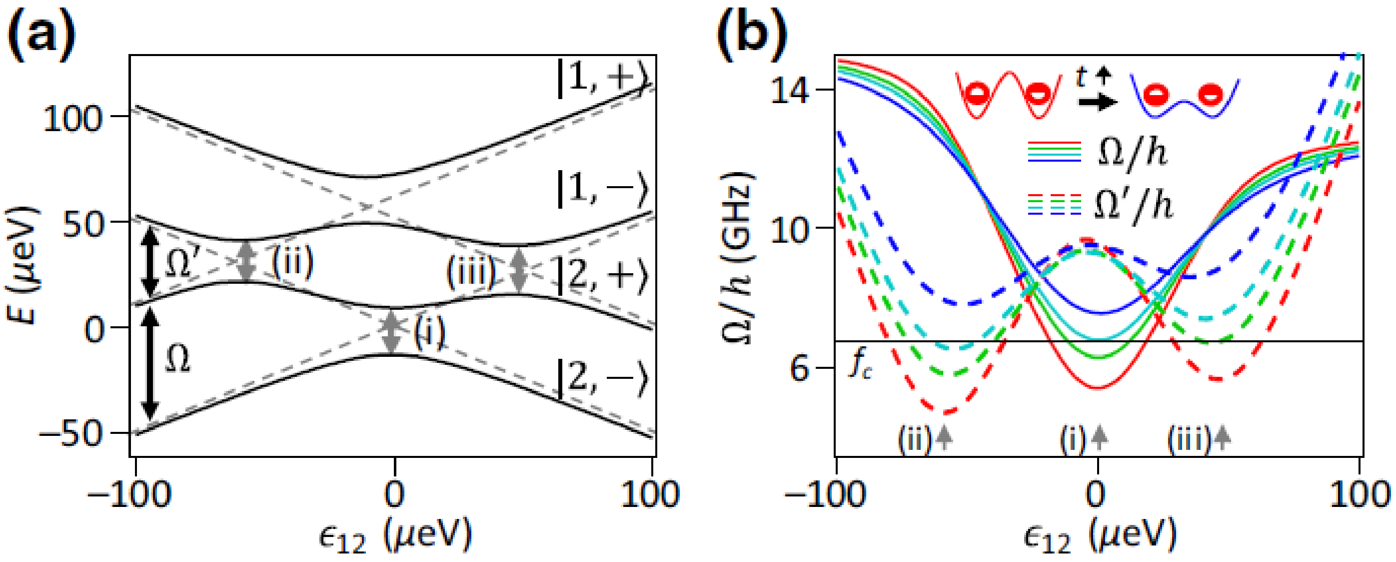

# Quantitative data analysis

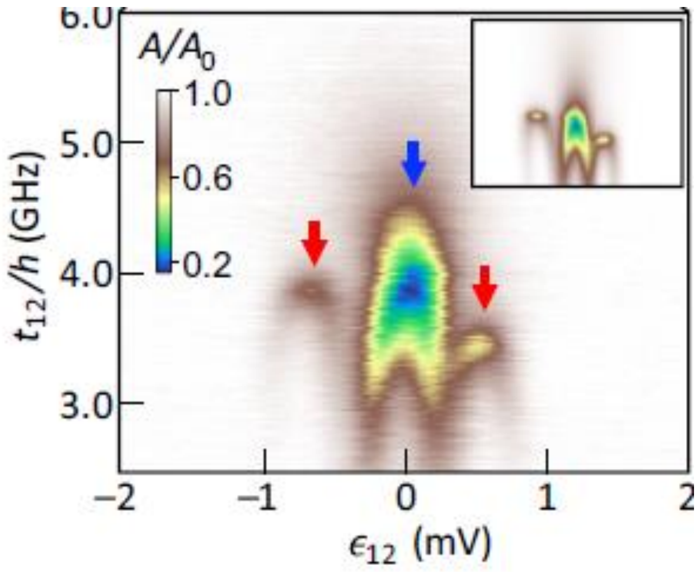


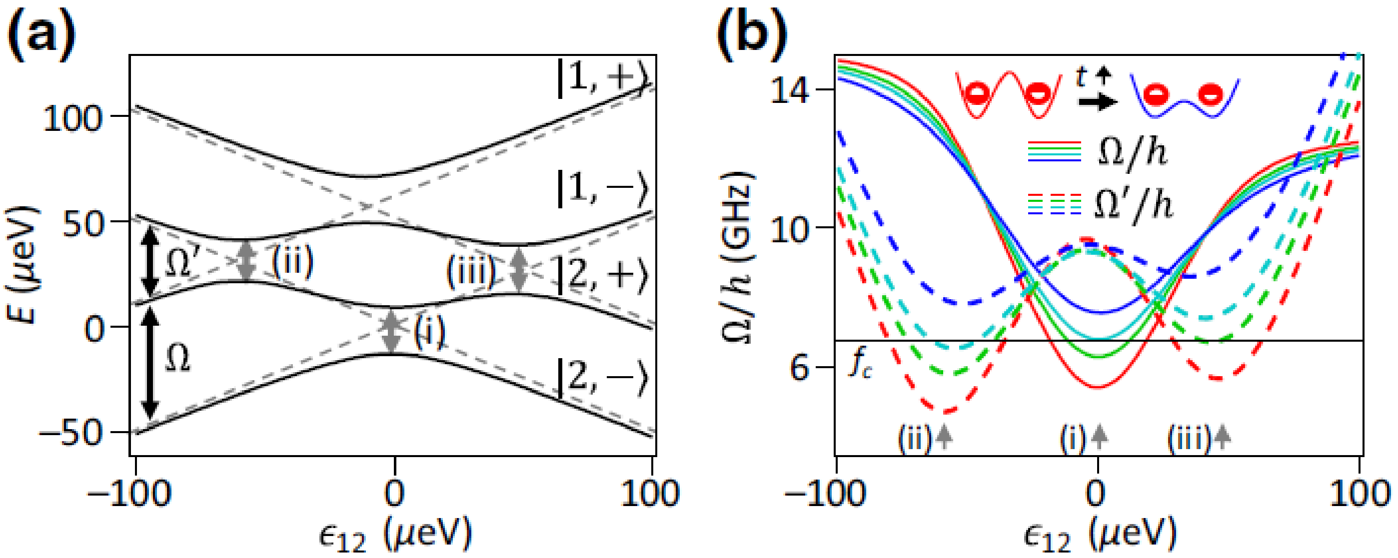


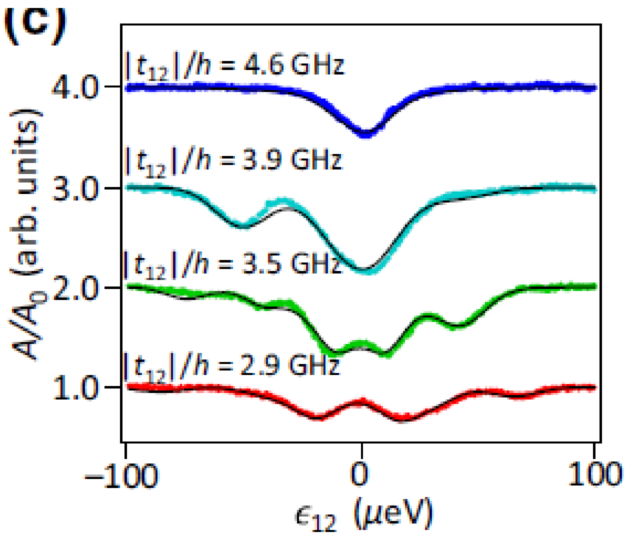


- **Analysis of traces of fixed $t_{12}$ ($V_B$)**
  - Numerical diagonalisation of Hamiltonian for each $\epsilon_{12}$
  - Feed resulting energies into cavity input-output theory
  - Add linear dependence $t_{12} = t_{12}(\epsilon = 0) + a_{12}\epsilon_{12}$ to account for asymmetry
  - Independently measure charge decoherence rate $\gamma_{12}$
  - Fit parameters:
    - Valley splittings $E_{V,i}$ - Intra valley-tunnelings $t_{12}(\epsilon_{12} = 0)$
    - Valley phase differences $\delta\Phi_{12}$ - Asymmetry $a_{12}$
    - Lever arms $\alpha_{ij}$ - Charge-cavity coupling rate $g_{12}$
    - Inhomogeneous broadening $\sigma_{12}$

# Results of data analysis

- Linear dependence between barrier gate and tunnel couplings

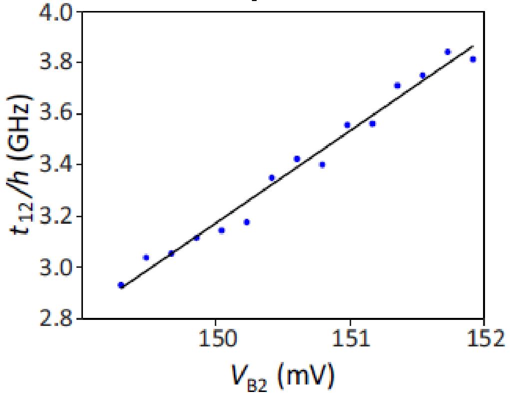


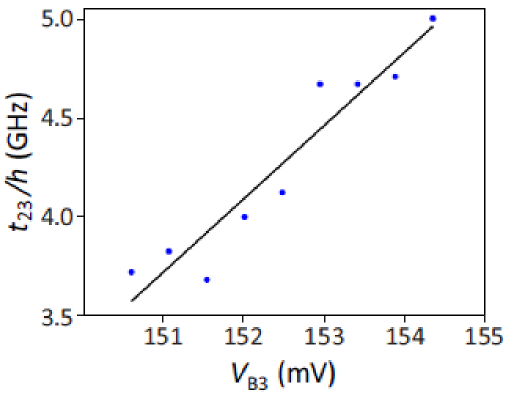

# Results of data analysis

- Linear dependence between barrier gate and tunnel couplings

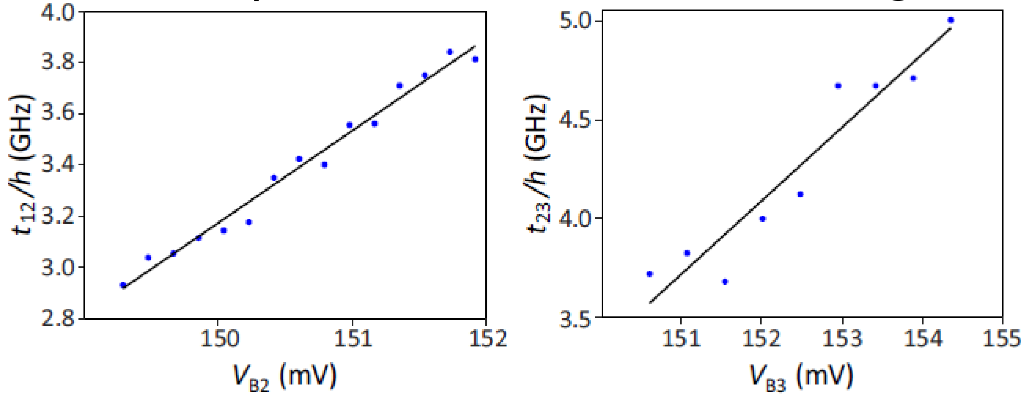


- Consistent extraction of valley splittings
  (1,0,0)-(0,1,0): $E_{V1} = 63\ \mu\text{eV}$, $E_{V2} = 53\ \mu\text{eV}$; (0,1,0)-(0,0,1): $E_{V2} = 50\ \mu\text{eV}$, $E_{V2} = 38\ \mu\text{eV}$

# Results of data analysis

- Linear dependence between barrier gate and tunnel couplings

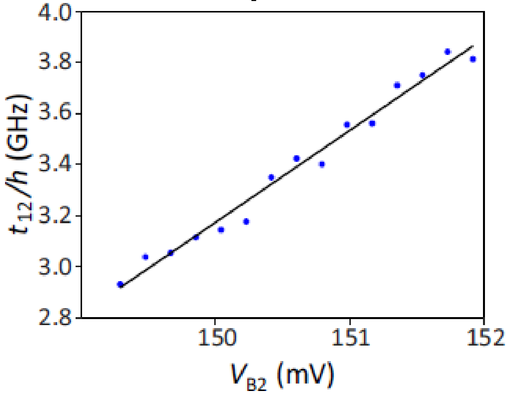


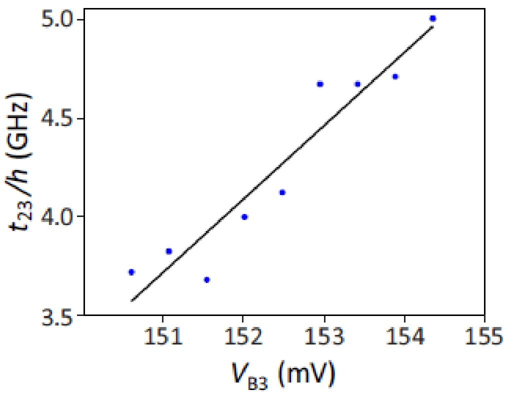


- Consistent extraction of valley splittings

  (1,0,0)-(0,1,0): $E_{V1} = 63\ \mu\text{eV}$, $E_{V2} = 53\ \mu\text{eV}$; (0,1,0)-(0,0,1): $E_{V2} = 50\ \mu\text{eV}$, $E_{V2} = 38\ \mu\text{eV}$
- Linear dependence between intra- and intervalley coupling

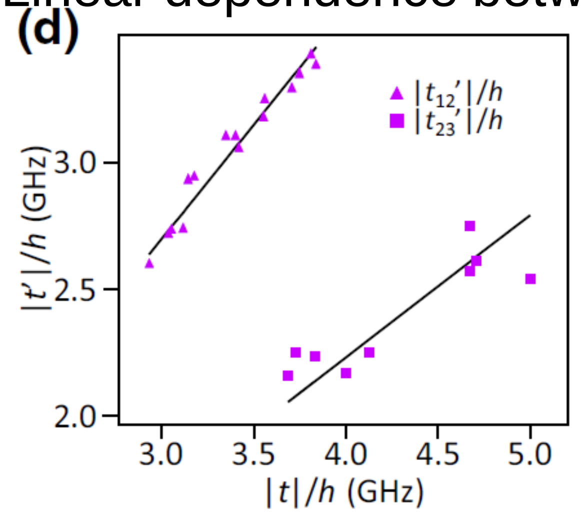

# Results of data analysis

- Linear dependence between barrier gate and tunnel couplings

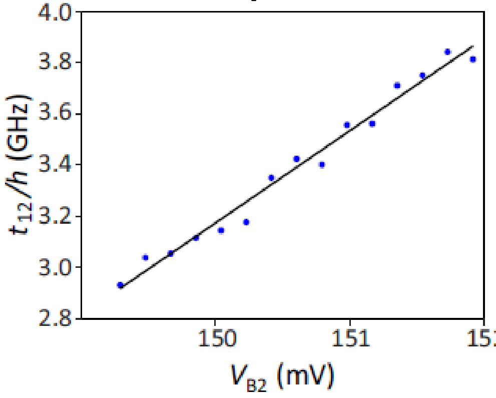


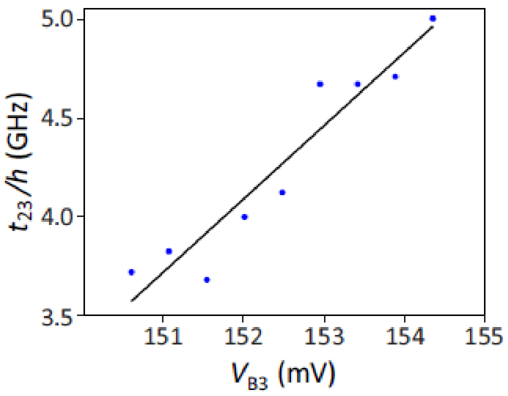


- Consistent extraction of valley splittings
  (1,0,0)-(0,1,0): $E_{V1} = 63$ μeV, $E_{V2} = 53$ μeV; (0,1,0)-(0,0,1): $E_{V2} = 50$ μeV, $E_{V2} = 38$ μeV
- Linear dependence between intra- and intervalley coupling

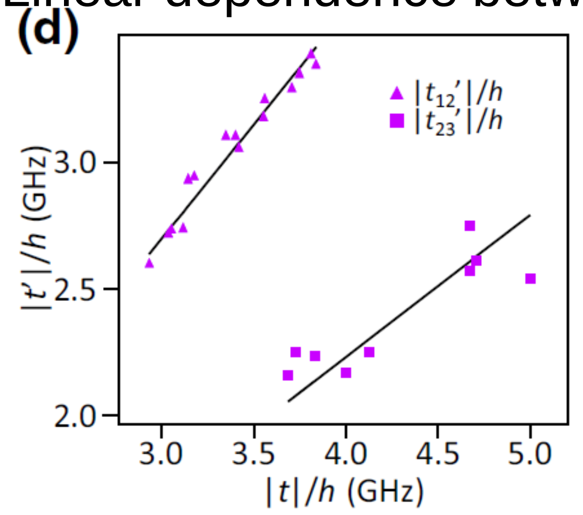


-> Large variations of valley phase $\delta\varphi_{ij} = 2\arctan(|t_{ij}/t'_{ij}|)$ between different dots (length scale 200 nm)

# Summary

- Circuit QED as sensitive measure for curvature in quantum dot energy levels

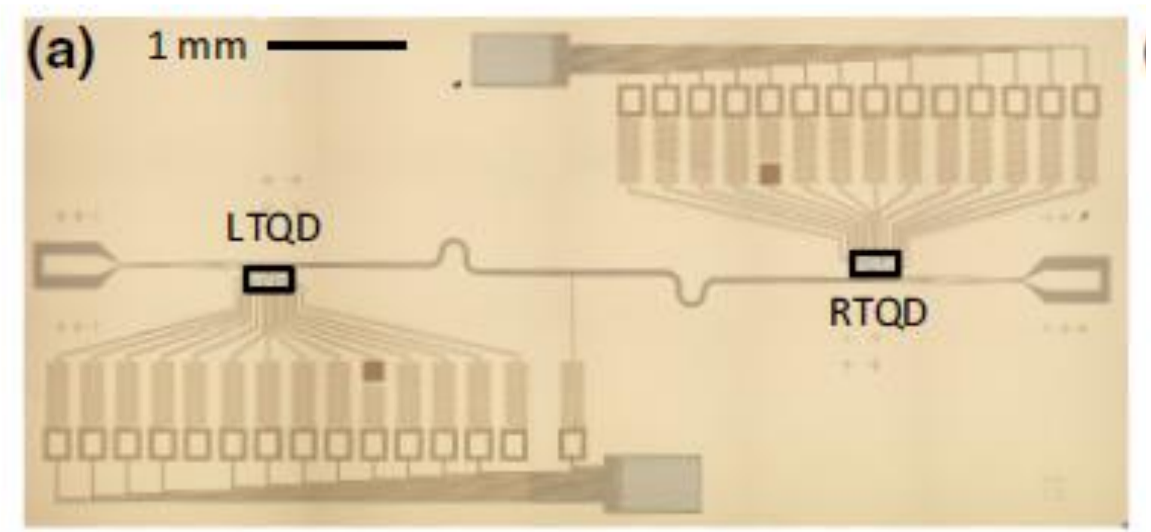


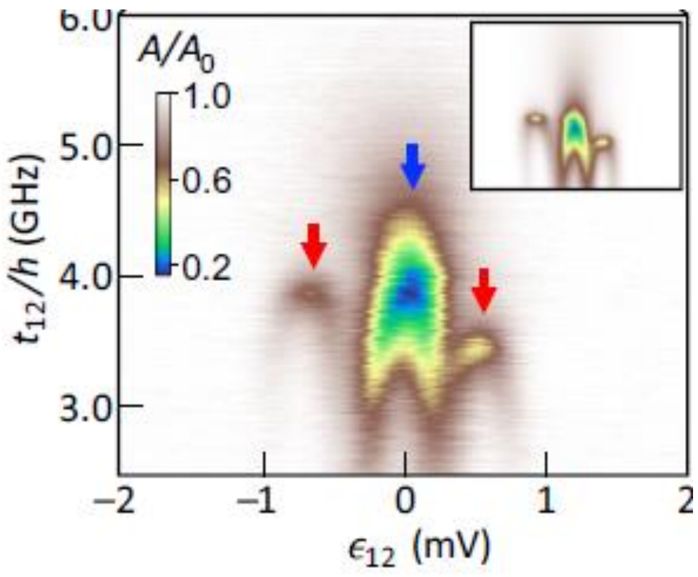


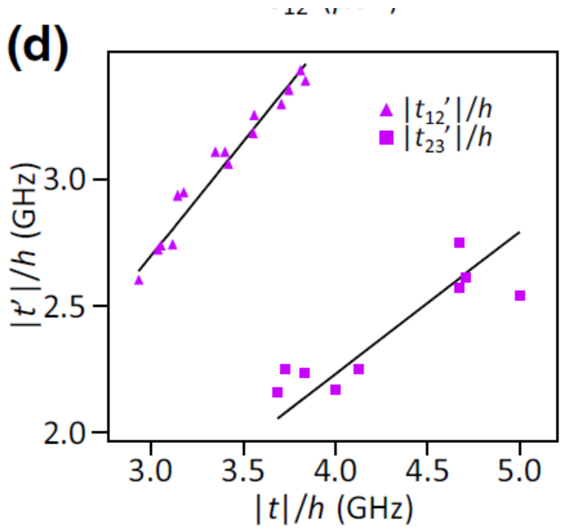

# Summary

- Circuit QED as sensitive measure for curvature in quantum dot energy levels
- Spectroscopical measurement of valley-splittings

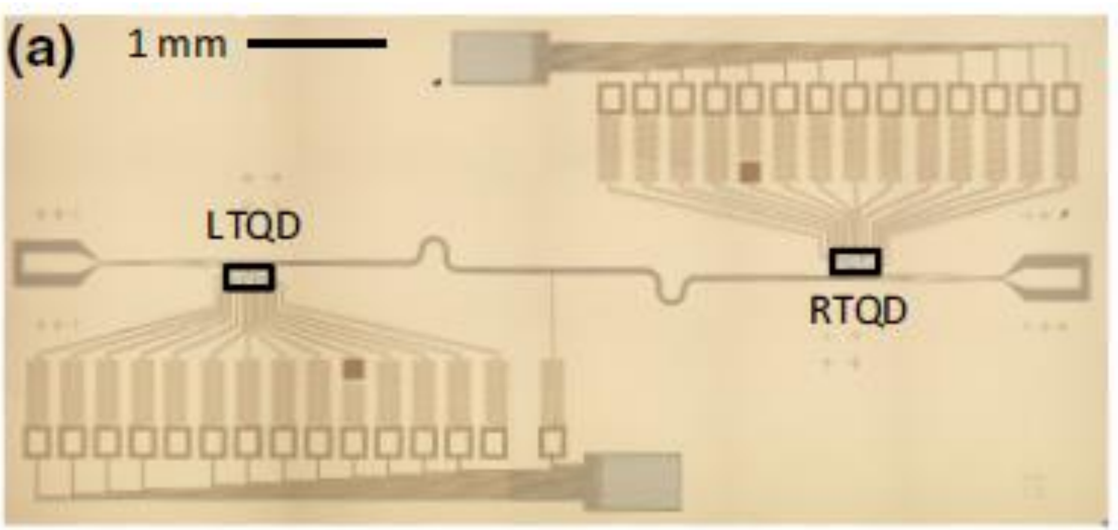


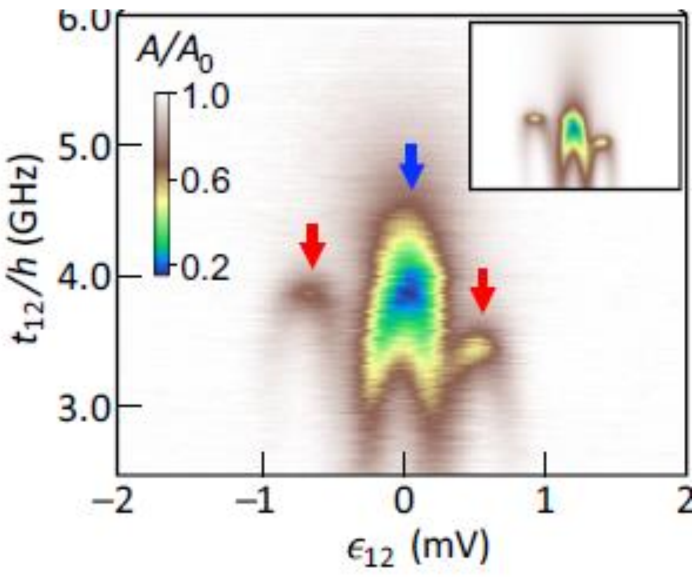


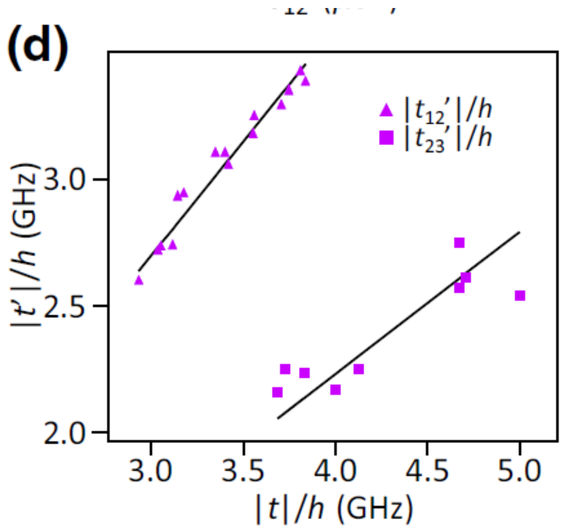

# Summary

- Circuit QED as sensitive measure for curvature in quantum dot energy levels
- Spectroscopical measurement of valley-splittings
- Consistent with theory, inter- and intravalley splitting scale linearly

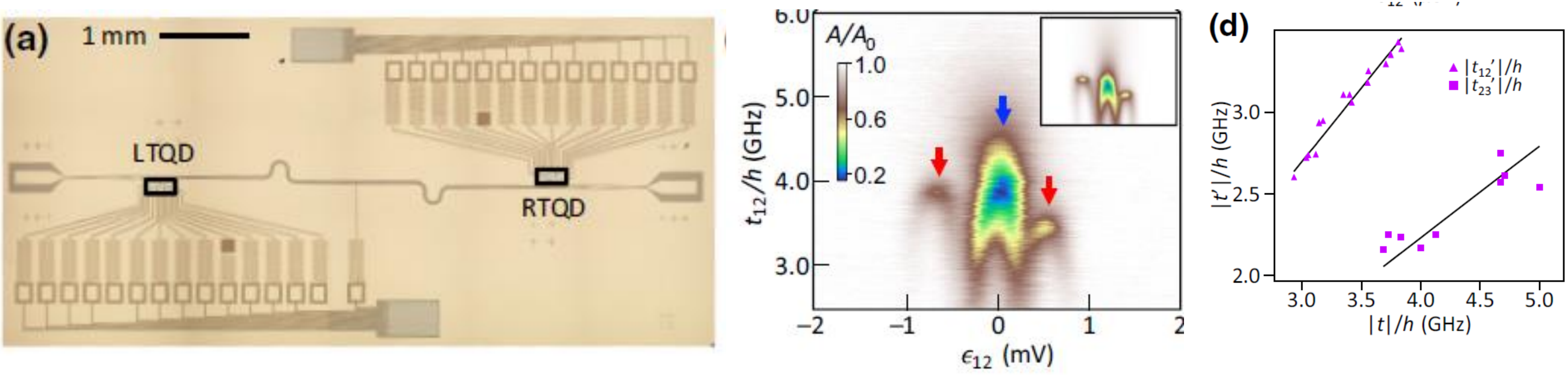

# Summary

- Circuit QED as sensitive measure for curvature in quantum dot energy levels
- Spectroscopical measurement of valley-splittings
- Consistent with theory, inter- and intravalley splitting scale linearly
- Observation of significant variations of the valley phase difference over approximately 200 nm
  - Improvement of Si/SiGe interface is needed

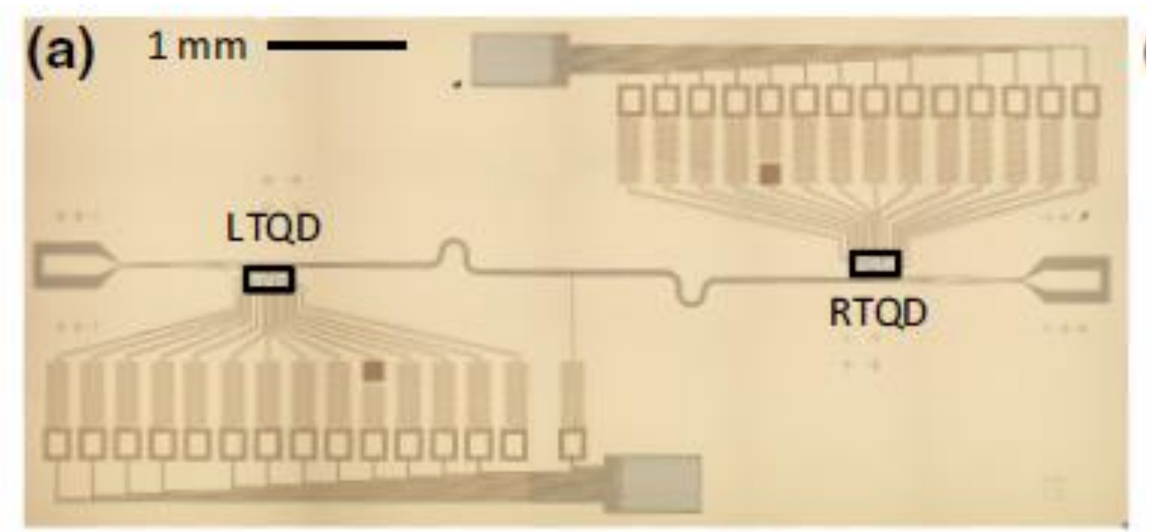


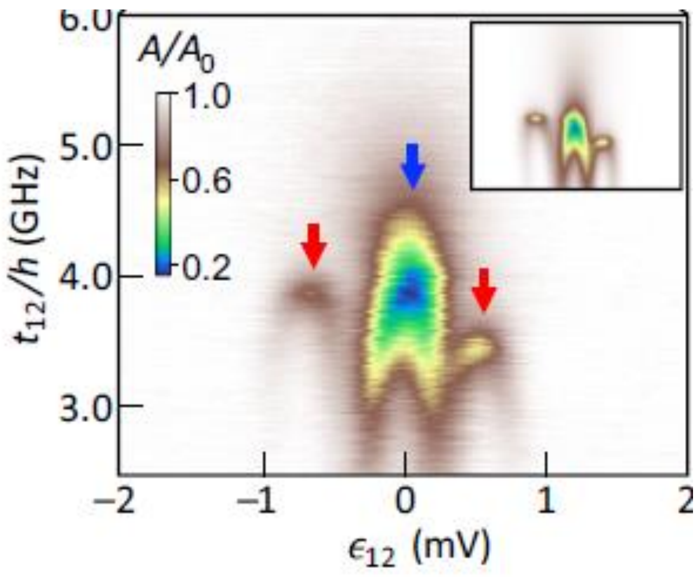


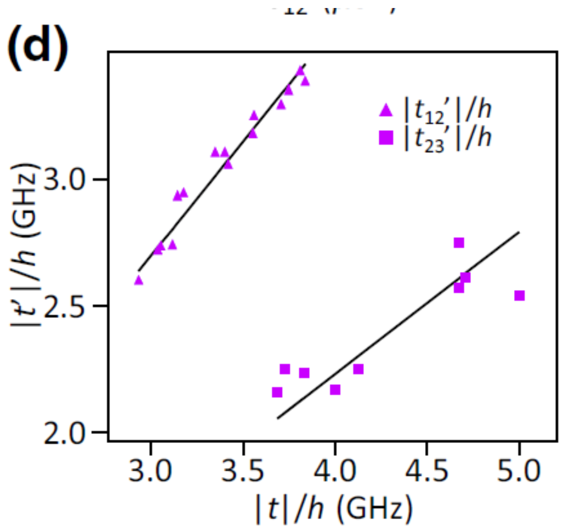

University of Basel

SNI
SWISS NANOSCIENCE INSTITUTE
EINE INITIATIVE DER UNIVERSITÄT BASEL UND DES KANTONS AARGAU

# Thank you
for your attention.